Chemical Communications

Dimetalla-Heterocyclic Carbenes: The Interplay of Chalcocarbonyl and Carbido Ligands

Received 00th January 20xx,
Accepted 00th January 20xx

DOI: 10.1039/x0xx00000x

www.rsc.org/

Harrison J. Barnett and Anthony F. Hill*

General Considerations

All reactions involving air-sensitive compounds were carried out under a dry and oxygen-free nitrogen atmosphere using standard Schlenk and vacuum line techniques, with the use of dried and degassed solvents.

NMR spectra were obtained at 298 K with Bruker Avance 400 (^{1}H at 400.1 MHz, ^{31}P at 161.9 MHz, and ^{13}C at 100.5 MHz), Bruker Avance 600 (^{1}H at 600.1 MHz, ^{31}P at 242.9 MHz, and ^{13}C at 192.5 MHz) or Bruker Avance 700 (^{1}H at 700.1 MHz, ^{31}P at 283.5 MHz, and ^{13}C at 176.1 MHz) spectrometers. Chemical shifts (δ) are reported in ppm and referenced internally to the solvent peak for ^{1}H and ^{13}C, and external H_3PO_4 reference for ^{31}P and Se_2Ph_2 for ^{77}Se NMR. The couplings for multiplicities of the NMR resonances, $^nJ_{AB}$, are reported in Hz. Spectra provided generally correspond to samples obtained directly from chromatography and may contain residual solvent as recrystallised samples often display reduced solubility.

ATR solid state spectra were obtained with a PerkinElmer FT-IR Spectrometer. Elemental microanalytical data when available were provided by the London Metropolitan University. High- and Low-Resolution Electrospray Ionisation Mass Spectrometry (ESI-MS) was performed by the ANU Research School of Chemistry mass spectrometry service, using acetonitrile for the matrix.

Crystallographic Details

Data for X-ray crystallography were collected with an Agilent SuperNova CCD diffractometer using Cu-Kα radiation (λ = 1.54184 Å) and the CrysAlisPRO software.[1] The structures were solved by direct or Patterson methods and refined by full-matrix least-squares on F^2 using the SHELXS or SHELXT and SHELXL programs.[2] Hydrogen atoms were located geometrically and refined using a riding model. Diagrams were produced using the CCDC visualisation program Mercury.[3]

The known compounds [Rh_2(u-C)Cl_2(dppm)$_2$] and [Rh_2(u-C)(μ-DMAD)Cl_2(dppm)$_2$] were prepared as described in the literature, and remaining reagents were obtained from commercial sources.

Computational Details

Computational studies were performed by using the SPARTAN18® suite of programs.[4] Geometry optimisation (gas phase) was performed at the DFT level of theory using the ωB97X-D dispersion-corrected functional of Head-Gordon.[5] The Los Alamos effective core potential type basis set (LANL2Dζ) of Hay and Wadt[6] was used for rhodium and iron; the Pople 6-31G* basis sets[7] were used for all other atoms. Frequency calculations were performed to confirm that the optimized structure was a minimum and also to identify vibrational modes of interest.

Reaction of [Rh_2(μ-C)Cl_2(PPh_3)$_4$] with CS_2.

In an NMR tube, a solution of [Rh_2(μ-C)Cl_2(PPh_3)$_4$] (0.010 g, 0.007 mmol) in $CDCl_3$ (0.5 mL) was treated with carbon disulfide (*ca* 0.01 mL, excess). The ^{31}P{^{1}H} NMR spectra (162 MHz) measured after 24 hours indicated complete and quantitative formation of [RhCl(CS)(PPh_3)$_2$] (δ_P = 31.0, $^1J_{RhP}$ = 142 Hz). Over the course of 48 hours, decomposition to PPh_3S ($\delta_P \approx 35$) is seen.

Synthesis of [Rh_2(μ-CS)Cl_2(μ-dppm)$_2$] (4)

To a flask containing [Rh_2(μ-C)Cl_2(μ-dppm)$_2$] (0.020 g, 0.017 mmol) in CH_2Cl_2 (20 mL), CS_2 was added (0.50 mL, 8.4 mmol). The resulting red solution was stirred for 5 hours, becoming dark green in colour. After this time the volatiles were removed *in vacuo* and the residue was subjected to column chromatography (10 x 1 cm silica gel column), eluting with neat CH_2Cl_2. A green band was collected, and the volatiles were removed under reduced pressure to give a green microcrystalline solid **4** (0.016 g, 0.015 mmol, 77%). IR (ATR, cm^{-1}): 1093 s ν_{CS}. ^{1}H NMR (400 MHz, $CDCl_3$, 298 K): δ_H = 3.02 (dq, *J* = 11, 4 Hz, 2 H, PCH_2), 3.58 (dt, *J* = 14, 5 Hz, 2 H, PCH_2), 7.07-7.09 (m, 8 H, C_6H_5), 7.21–7.24 (m, 4 H, C_6H_5),

a. Research School of Chemistry, Australian National University, Canberra, Australian Capital Territory, ACT 2601, Australia.
†Corresponding author: Email: a.hill@anu.edu.au
Electronic Supplementary Information (ESI) available: Synthetic procedures, spectroscopic and crystallographic data. See DOI: 10.1039/x0xx00000x. CCDC 2013308 - 2013311 contain the supplementary crystallographic data for this paper. These data can be obtained free of charge from The Cambridge Crystallographic Data Centre.

7.31–7.32 (m, 12 H, C_6H_5), 7.68 (br s, 16 H, C_6H_5). $^{13}C\{^1H\}$ NMR (151 MHz, $CDCl_3$, 298 K): δ_C = 27.4 (t, $^1J_{CP}$ = 10 Hz, PCH_2), 128.1, 128.2, 129.9, 130.6, 132.5, 136.1 (C_6H_5). The quaternary thiocarbonyl resonance, was not detected due to high multiplicity (AM_2X_4 system) and low intensity and solubility. $^{31}P\{^1H\}$ NMR (162 MHz, $CDCl_3$, 298 K): δ_P = 17.2 (d, $^1J_{RhP}$ = 118 Hz). MS (ESI, +ve ion, *m/z*): Found: 1052.98954 $[M–Cl]^+$. Calcd for $C_{51}H_{44}{}^{35}ClP_4{}^{103}Rh_2S$ $[M–Cl]^+$: 1052.99128. Anal. Found: C, 52.86; H, 3.79%. Calcd for $C_{51}H_{44}Cl_2P_4Rh_2.CH_2Cl_2$: C, 53.18; H, 3.95%. A crystal of a toluene solvate suitable for structure determination was grown by slow evaporation of CH_2Cl_2 from a toluene solution. *Crystal data for* $(C_{51}H_{44}Cl_2P_4Rh_2S)_2\cdot(C_7H_8)_{2.5}$, ($M_w$ = 2409.37 gmol^{-1}): triclinic, space group *P*-1 (No. 2), *a* = 16.3139(3), *b* = 19.5375(3), *c* = 22.4893(4) Å, *α* = 71.332(2)°, *β* = 72.996(2)°, *γ* = 79.948(2)°, *V* = 6468.1(2) Å^3, *Z* = 2, *T* = 150.0(1) K, μ(Cu Kα) = 22.258 mm^{-1}, D_{calc} = 1.237 Mgm^{-3}, gold plate 0.40 x 0.162 x 0.082 mm, 25086 reflections measured (7.2° ≤ 2Θ ≤ 141.6°), 19891 unique (R_{int} = 0.067) which were used in all calculations. The final R_1 was 0.073 ($I > 2\sigma(I)$) and wR_2 was 0.225 (all data) for 1235 refined parameters with 263 restraints. CCDC 2013308.

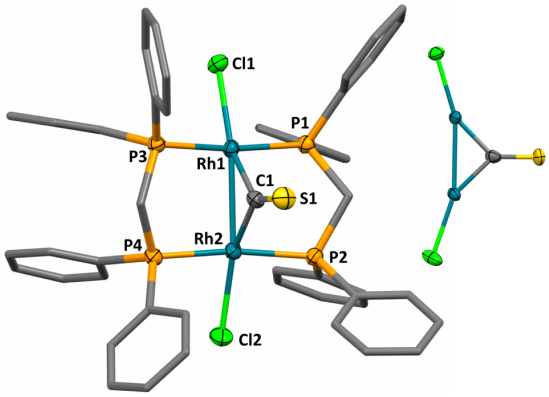

Figure S1. Molecular structure **4** in a crystal of **4**.$(PhMe)_{0.5}$ (50% displacement ellipsoids, solvent and hydrogen atoms omitted and dppm groups simplified, one of two crystallographically independent molecules shown). Selected bond lengths (Å) and angles (°): Rh1–Rh2 2.7059(4), Rh1–Cl1 2.3591(10), Rh1–C1 1.914(4), Rh2–Cl2 2.3659(11), Rh2–C1 1.913(4), S1–C1 1.619(4), Cl1–Rh1–Rh2 162.51(3), C1–Rh1–Rh2 44.98(12), C1–Rh1–Cl1 152.50(13), Cl2–Rh2–Rh1 161.84(4), C1–Rh2–Rh1 45.02(13), C1–Rh2–Cl2 153.11(13), Rh2–C1–Rh1 90.00(19), S1–C1–Rh1 134.6(2), S1–C1–Rh2 135.4(2). Inset show view orthogonal to the Rh_2C plane.

Synthesis of $[Rh_2(\mu\text{-CSe})Cl_2(\mu\text{-dppm})_2]$ (5)

To a flask containing $[Rh_2(\mu\text{-C})Cl_2(\mu\text{-dppm})_2]$ (0.050 g, 0.047 mmol) in CH_2Cl_2 (50 mL), excess grey selenium was added (0.014 g, 0.173 mg.atom). The resulting red solution was stirred for 15 hours, becoming dark green in colour. After this time volatiles were removed *in vacuo* and the residue was subjected to column chromatography (10 x 1 cm silica gel column), eluting with neat CH_2Cl_2. A green band was collected, and the volatiles were removed under reduced pressure to give a green microcrystalline solid **5** (0.028 g, 0.025 mmol, 52%). IR (ATR, cm^{-1}): 957 s ν_{CSe}. ^1H NMR (400 MHz, $CDCl_3$, 298 K): δ_H = 2.96 (br. d, *J* = 14 Hz, 2 H, PCH_2), 3.68 (dt, *J* = 14, 4 Hz, 2 H, PCH_2), 7.04-7.08 (m, 7 H, C_6H_5), 7.15–7.23 (m, 5 H, C_6H_5), 7.31–7.33 (m, 12 H, C_6H_5), 7.66-7.71 (m, 16 H, C_6H_5). $^{13}C\{^1H\}$ NMR (151 MHz, $CDCl_3$, 298 K): δ_C = 26.3 (t, $^1J_{CP}$ = 11 Hz, PCH_2), 128.1, 128.2, 129.9, 130.6, 132.5, 136.1 (C_6H_5). The selenocarbonyl resonance was not directly detected due to high multiplicity (AM_2X_4) and low intensity and solubility. $^{31}P\{^1H\}$ NMR (162 MHz, $CDCl_3$, 298 K): δ_P = 14.7 (d, $^1J_{RhP}$ = 119 Hz). $^{77}Se\{^1H\}$ NMR (134 MHz, $CDCl_3$, 298 K) δ_{Se} = not detected due to high splitting. MS (ESI, +ve ion, *m/z*): Found: 1100.9379 $[M–Cl]^+$. Calcd for $C_{51}H_{44}{}^{35}ClP_4{}^{103}Rh_2{}^{80}Se$ $[M–Cl]^+$: 1100.9360. A crystal of a toluene solvate suitable for structure determination was grown by slow evaporation of CH_2Cl_2 from a toluene solution. *Crystal data for* $2(C_{51}H_{44}Cl_2P_4Rh_2Se)\cdot3(C_7H_8)$ (M_w = 2549.24 gmol^{-1}): triclinic, space group *P*-1 (No. 2), *a* = 16.2884(4), *b* = 20.0388(5), *c* = 22.3244(6) Å, *α* = 70.671(2)°, *β* = 75.071(2)°, *γ* = 80.200(2)°, *V* = 6615.0(3) Å^3, *Z* = 2, *T* = 150.0(1) K, μ(Cu Kα) = 22.258 mm^{-1}, D_{calc} = 1.280 Mgm^{-3}, dark green block 0.27 x 0.11 x 0.07 mm, 38393 reflections measured (7.0° ≤ 2Θ ≤ 141.8°), 18074 unique (R_{int} = 0.036) which were used in all calculations. The final R_1 was 0.083 ($I > 2\sigma(I)$) and wR_2 was 0.260 (all data) for 1201 refined parameters with 459 restraints. CCDC 2013309.

Synthesis of $[Rh_2(\mu\text{-CS})Cl_2(\mu\text{-DMAD})(\mu\text{-dppm})_2]$ (7)

Method A: To a flask containing $[Rh_2(\mu\text{-CS})Cl_2(dppm)_2]$ (**4**: 0.050 g, 0.047 mmol) was added CH_2Cl_2 (10 mL) followed by dimethylacetylenedicarboxylate (DMAD: 0.10 mL, 1.7 mmol). The resulting green solution was stirred for 60 minutes at room temperature, turning red in colour. Over this time a red precipitate formed and this was isolated by filtration and washed with hexane to remove unreacted DMAD. Drying *in vacuo* gave a red powder of pure **7** (0.046 g, 0.037 mmol, 79%). IR (ATR, cm^{-1}): 1720 br, s ν_{CO}, 1249 br, s ν_{CS}. ^1H NMR (400 MHz, $CDCl_3$, 298 K): δ_H = 2.41 (s, 6H, CH_3), 2.88 (br. d, $^2J_{HH}$ = 12 Hz, PCH_2), 3.95 (dp, *J* = 18, 6 Hz, PCH_2), 7.01 (t, *J* = 8 Hz, 9 H, C_6H_5), 7.17 (t, *J* = 7 Hz, 5 H, C_6H_5), 7.30–7.35 (m, 16 H, C_6H_5), 7.73 (q, *J* = 5 Hz, 8 H, C_6H_5) 7.83 (br. d, *J* = 6 Hz, C_6H_5). $^{13}C\{^1H\}$ NMR (151 MHz, $CDCl_3$, 298 K): δ_C = 16.6 (t, $^1J_{CP}$ = 11 Hz, PCH_2), 50.3 (OCH_3), 125.7, 128.1, 128.5, 130.2, 130.6, 132.4, 135.2 (C_6H_5), 164.5 (CO_2; HMBC with δ_H = 2.43). $^{31}P\{^1H\}$ NMR (162 MHz, $CDCl_3$, 298 K): δ_P = 7.09 (d, $^1J_{RhP}$ = 133 Hz). MS (ESI, +ve ion, *m/z*): Found: 1195.0172. Calcd for $C_{57}H_{50}{}^{35}ClO_4P_4{}^{103}Rh_2S$ $[M–Cl]^+$: 1195.0179. A crystal of a chloroform solvate of the aquo adduct suitable for structure determination was grown by slow evaporation of a wet $CHCl_3$/petrol mixture. *Crystal data for* $C_{57}H_{52}Cl_2O_5P_4Rh_2S\cdot CHCl_3$ (M = 1369.01 gmol^{-1}): monoclinic, space group $P2_1/c$ (no. 14), *a* = 12.7306(2), *b* = 15.6417(3), *c* = 30.6406(4) Å, *β* = 92.455(1)°, *V* = 6095.81(17) Å^3, *Z* = 4, *T* = 150.0(1) K, μ(Cu Kα) = 22.258 mm^{-1}, D_{calc} = 1.492 Mgm^{-3}, red plate 0.125 x 0.055 x 0.032 mm, 11380 reflections measured (8.0° ≤ 2Θ ≤ 142.2°), 9442 unique (R_{int} = 0.028) which were used in all calculations. The final R_1 was 0.049 ($I > 2\sigma(I)$) and wR_2 was 0.128 (all data) for 679 refined parameters without restraints. CCDC 2013310.

Method B: To a flask containing [$Rh_2(\mu_2$-C)(μ_2-DMAD)Cl_2(dppm)$_2$] (0.040 g, 0.033 mmol) was added CH_2Cl_2 (10 mL) followed by S_8 (0.023 g, 0.090 mmol). The resulting red suspension was stirred for 15 hours at room temperature, turning dark red as the starting material dissolved to give a clear solution. The solution was concentrated under reduced volume and subjected to a silica gel column (10 x 1 cm). Eluting with a with 5% mixture of THF in CH_2Cl_2 provided the red band which was freed of volatiles to afford the desired product **7** (0.018 g, 0.015 mmol, 44%). The product was identified comparison of ESI-MS and ^{31}P NMR spectroscopic data with those for a sample prepared as described above.

Synthesis of [$Rh_2(\mu$-CSe)$Cl_2(\mu$-DMAD)(μ-dppm)$_2$] (8)

Method A: To a flask containing [$Rh_2(\mu_2$-C)(μ_2-DMAD)Cl_2(μ-dppm)$_2$] (0.100 g, 0.083 mmol) was added CH_2Cl_2 (10 mL) followed by grey selenium (0.009 g, 0.11 mg.atom). The resulting red suspension was stirred for 24 hours at room temperature. The supernatant was decanted to remove excess suspended selenium, and the red solution concentrated under reduced pressure to ca 1 mL. Subjecting the solution to a silica gel column (1 x 10 cm), a pink band was eluted using a mixture of 5% THF in CH_2Cl_2. A pink powder precipitated upon addition of petroleum spirits and drying *in vacuo* gave a pink powder of pure **8** (0.015 g, 0.012 mmol, 14%). IR (ATR, cm^{-1}): 1718 br, s ν_{CO}, 893, s ν_{CSe}. ^{1}H NMR (400 MHz, $CDCl_3$, 298 K): δ_H = 2.46 (s, 6H, OCH_3), 2.79-2.86 (m, 2H, PCH_2), 3.79-3.85 (m, 2H, PCH_2), 7.03,7.34, 7.72, 7.83, 8.04 (m x 5, 40 H, C_6H_5). ^{13}C{^{1}H} NMR (151 MHz, $CDCl_3$, 298 K): δ_C = 16.7 (PCH_2), 50.4 (OCH_3), 125.7, 128.1, 128.4, 130.2, 130.6, 132.6, 132.7, 135.3, 135.9 (dppm C_6H_5), 164.7 (HMBC with δ_H = 2.48). ^{31}P{^{1}H} NMR (162 MHz, $CDCl_3$, 298 K): δ_P = 4.11 (d, $^1J_{RhP}$ = 131 Hz). ^{77}Se{^{1}H} NMR (134 MHz, $CDCl_3$, 298 K) δ_{Se} = not detected due to high splitting. MS (ESI, +ve ion, *m/z*): Found: 1242.9637. Calcd for $C_{57}H_{50}{}^{35}ClO_4P_4{}^{103}Rh_2Se$ [M–Cl]$^+$: 1242.9629. A crystal suitable for structure determination was grown by slow evaporation of a wet CH_2Cl_2/toluene mixture. *Crystal data for* $C_{57}H_{52}Cl_2O_5P_4Rh_2Se\cdot0.5(CH_2Cl_2)\cdot C_7H_8$ (M = 1431.14 gmol^{-1}): monoclinic, space group $P2_1/c$ (No. 14), a = 12.4786(2), b = 15.7365(2), c = 31.0651(4) Å, β = 91.657(1)°, V = 6097.69(15) Å^3, Z = 4, T = 150.0(1) K, μ(Cu Kα) = 22.258 mm^{-1}, D_{calc} = 1.559 Mgm^{-3}, red plate 0.305 x 0.179 x 0.066, 11460 reflections measured (7.0° ≤ 2Θ ≤ 141.8°), 9756 unique (R_{int} = 0.035) which were used in all calculations. The final R_1 was 0.058 ($I > 2\sigma(I)$) and wR_2 was 0.152 (all data) for 734 refined parameters without restraints. CCDC 2013307.

Method B: To a flask containing [$Rh_2(\mu_2$-CSe)Cl_2(dppm)$_2$] (**5**) (0.040 g, 0.035 mmol) was added CH_2Cl_2 (20 mL). To this green solution was added DMAD (0.05 mL, 0.4 mmol). The resulting dark green solution was stirred for 24 hours at room temperature, turning pink in colour. The solution was concentrated under reduced volume and subjected to a silica gel column. Eluting a red band with 5% THF in CH_2Cl_2 provided the pink product **8** (0.038 g, 0.030 mmol, 84 %). Product was confirmed through ESI-MS and ^{31}P NMR spectroscopy, matching those mentioned above. Despite numerous attempts at purification through chromatography and crystallization, the impurity of polymerized DMAD remained present in the NMR using Method B, though the compound could be accurately characterized using ^{1}H-^{1}H COSY, ^{1}H-^{13}C HSQC and HMBC NMR.

1 Agilent, CrysAlis PRO, Agilent Technologies Ltd, Yarnton, Oxfordshire, England, 2014.

2 (a) G. Sheldrick, *Acta Crystallogr. Sect. A: Found. Crystallogr.*, 2008, **64**, 112-122; (b) G. M. Sheldrick, *Acta Crystallogr. Sect. C: Cryst. Struct. Commun.*, 2015, **71**, 3-8.

3 21. (a) C. F. Macrae, P. R. Edgington, P. McCabe, E. Pidcock, G. P. Shields, R. Taylor, M. Towler and J. van de Streek, *J. Appl. Crystallogr.*, 2006, **39**, 453-457; (b) C. F. Macrae, I. J. Bruno, J. A. Chisholm, P. R. Edgington, P. McCabe, E. Pidcock, L. Rodriguez-Monge, R. Taylor, J. van de Streek and P. A. Wood, *J. Appl. Crystallogr.*, 2008, **41**, 466-470

4 *Spartan 18*® (2018) Wavefunction, Inc., 18401 Von Karman Ave., Suite 370 Irvine, CA 92612 U.S.A.

5 J.-D. Chai and M. Head-Gordon, *Phys. Chem. Chem. Phys.* 2008, **10**, 6615.

6 (a) P. J. Hay and W.R. Wadt, *J. Chem. Phys.*, 1985, **82**, 270-283. (b) W. R. Wadt and P. J. Hay, *J. Chem. Phys.,* 1985, **82**, 284-298. (c) P. J. Hay, W. R. Wadt, *J. Chem. Phys.,* 1985, **82**, 299-310.

7 W. J. Hehre, R. Ditchfeld and J. A. Pople, *J. Chem. Phys.*, 1972, **56**, 2257-2261.

Table S1. Experimental and Computational[a] CSe-associated data for bridging CSe Ligands

Complex	ν_{CSe} [cm^{-1}]	r_{CSe} [Å]	Se Charge	C–Se Bond Order
Experimental[b]				
$Rh_2(\mu$-CSe)Cl_2(dppm)$_2$	957	1.747(8)		
Rh2(μ-CSe)Cl_2(μ-DMAD)(dppm)$_2$	1000[c]	1.785(6)		
Calculated[a]				
$Rh_2(\mu$-CSe)Cl_2(CO)$_6$	1020	1.703	+0.35	2.14
$Rh_2(\mu$-CSe)Cl_2(CO)$_4$	1032	1.706	+0.31	2.06
$Rh_2(\mu$-CSe)Cl_2(dmpm)$_2$	974	1.756	–0.03	1.74
$Rh_2(\mu$-CSe)Cl_2(dHpm)$_2$	990	1.742	+0.06	1.83
$Rh_2(\mu$-CSe)Cl_2(μ-HCCH)(dmpm)$_2$	815	1.813	–0.18	1.501

[a] Calculated at the DFT: ωB96X-D/6-31G*/LANL2Dζ level of theory in the gas phase. Scaling factor = 0.9420. [b] Solid-state data acquired in ATR mode. [c]Ambiguous assignment due to weak intensity.

Table S2 Selected structural data for the complexes $[Rh_2(\mu\text{-CA})Cl_2(dRpm)_2]$

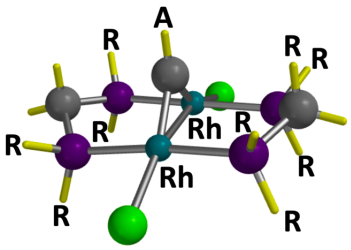

X =	R =	Rh–Rh [Å]	Rh–C [Å]	Rh–Cl [Å]	Rh–C–X [°]
O[a]	Ph	2.726(3)	1.90(3), 1.90(3)	2.348(8), 2.348(8)	136(2), 133(2)
Mean		*2.726*	*1.90*	*2.348*	*135*
S	Ph	2.7058(6)	1.912(6), 1.920(6)	2.3608(14), 2.3657(16)	135.1(4), 135.1(4)
		2.7184(6)	1.906(6), 1.922(6)	2.3579(14), 2.3612(16)	135.5(3), 134.0(3)
Mean		*2.7121*	*1.915*	*2.3614*	*134.9*
Se	Ph	2.7575(9)	1.914(10), 1.927(8)	2.351(2),2.347(2)	136.0(5), 132.4(5)
		2.7933(9)	1.935(10), 1.963(10)	2.346(3), 2.357(3)	133.9(5), 134.3(6)
Mean		*2.7754*	*1.935*	*2.350*	*134.2*
O[b]	Me	2.741	1.967, 1.965	2.425, 2.426	135.5, 136.1
Mean		*2.741*	*1.966*	*2.426*	*135.8*
S[b]	*Me*	*2.727*	*1.930, 1.932*	*2.426, 2.429*	*135.0, 135.1*
Mean		*2.727*	*1.931*	*2.428*	*135.1*
Se[b]	*Me*	*2.724*	*1.921, 1.921*	*2.428, 2.427*	*134.9, 134.7*
Mean		*2.724*	*1.921*	*2.428*	*134.8*
Se[b]	*H*	*2.735*	*1.934, 1.933*	*2.394, 2.394*	*134.9, 135.1*
Mean		*2.735*	*1.934*	*2.394*	*135.0*

[a]Taken from L. Gelmini, D. W. Stephan and S. J. Loeb, *Inorg. Chim. Acta*, 1985, **98**, L3-L6. [b]Calculated for gas-phase geometry optimised at the DFT: ωB97X-D/6-31G*/LANL2Dζ level of theory.

Table S3. Experimental crystallographic data

	4	5	7	8
Crystal data for	$(C_{51}H_{44}Cl_2P_4Rh_2S)_2\cdot(C_7H_8)_{2.5}$	$2(C_{51}H_{44}Cl_2P_4Rh_2Se)\cdot3(C_7H_8)$	$C_{57}H_{52}Cl_2O_5P_4Rh_2S\cdot CHCl_3$	$C_{57}H_{52}Cl_2O_5P_4Rh_2Se\cdot0.5(CH_2Cl_2)\cdot C_7H_8$
M_w	2409.37 gmol^{-1}	2549.24 gmol^{-1}	1369.01 gmol^{-1}	1431.14 gmol^{-1}
Crystal class	Triclinic	Triclinic	Monoclinic	Monoclinic
Space group	*P*-1 (No. 2)	*P*-1 (No. 2)	$P2_1/c$ (no. 14)	$P2_1/c$ (No. 14)
a	*a* = 16.3139(3) Å	16.2884(4) Å	12.7306(2) Å	12.4786(2) Å
b	*b* = 19.5375(3) Å	20.0388(5) Å	15.6417(3) Å	15.7365(2) Å
c	22.4893(4) Å	22.3244(6) Å	30.6406(4) Å	31.0651(4) Å
α	71.332(2)°	70.671(2)°	0	0
β	72.996(2)°	75.071(2)°	92.455(1)°	91.657(1)°
γ	79.948(2)°	80.200(2)°	0	0
V	6468.1(2) Å^3	6615.0(3) Å^3	6095.81(17) Å^3	6097.69(15) Å^3
Z	2	2	4	4
T	150.0(1)	150.0(1) K	150.0(1) K	150.0(1)
μ	22.258 mm^{-1} (Cu Kα)	22.258 mm^{-1} (Cu Kα)	22.258 mm^{-1} (Cu Kα)	22.258 mm^{-1} (Cu Kα)
D_{calc}	1.237 Mgm^{-3}	1.280 Mgm^{-3}	1.492 Mgm^{-3}	1.559 Mgm^{-3}
crystal aspect	gold plate	dark green block	red plate	red plate
Dimensions	0.40 x 0.162 x 0.082 mm	0.27 x 0.11 x 0.07 mm	0.125 x 0.055 x 0.032 mm	0.305 x 0.179 x 0.066 mm
Reflections (measured)	25086	38393	11380	11460
2Θ range	7.2° ≤ 2Θ ≤ 141.6°	7.0° ≤ 2Θ ≤ 141.8°	8.0° ≤ 2Θ ≤ 142.2°	7.0° ≤ 2Θ ≤ 141.8°
Reflections (unique)	19891	18074	9442	9756
R_{int}	0.067	0.036	0.028	R_{int} = 0.035
R_1 ($I > 2\sigma(I)$)	0.073	0.083	0.049	0.058
wR_2 (all data)	0.225	0.260	0.128	0.152
Refined parameters	1235	1201	679	734
Restraints	263	459	0	0
CCDC	2013308	2013309	2013310.	2013307

Geometry Optimisation for [Rh(μ-CO)Cl_2(dmpm)$_2$]

DFT: ωB97X-D/6-31G*/LANL2Dζ/gas phase

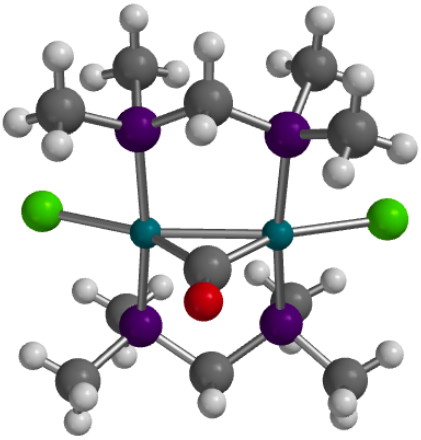

Figure S2

Table S3. Cartesian Coordinates

Atom	x	y	z
Rh	-1.118278	0.066326	0.803386
Rh	1.131249	0.218132	-0.754548
Cl	3.003864	-0.431048	-2.151960
Cl	-3.068575	-0.809443	1.949070
O	0.132487	2.693842	0.446914
P	0.038346	-0.305014	2.788333
P	-0.021436	0.622760	-2.734750
P	-2.516075	0.289838	-1.046692
P	2.514805	-0.312156	1.042833
C	-1.773820	1.144243	-2.503391
H	-1.749884	2.209994	-2.244858
H	-2.373898	1.027841	-3.413203
C	0.071039	1.531331	0.256358
C	1.836966	0.089031	2.710748
H	1.922322	1.177535	2.815632
H	2.407477	-0.377236	3.522304
C	4.152710	0.502218	1.062862
H	4.759890	0.169544	1.911195
H	4.014827	1.585775	1.112500
H	4.658859	0.265043	0.123494
C	2.931554	-2.094052	1.117697
H	3.541957	-2.334407	1.994565
H	3.480631	-2.339346	0.204287
H	2.016212	-2.690525	1.128543
C	-0.039416	-2.017548	3.427913
H	0.503814	-2.115606	4.373490
H	0.372112	-2.715197	2.695018
H	-1.093947	-2.265674	3.575178
C	-0.557461	0.695965	4.198362
H	0.000917	0.482886	5.115711
H	-1.617110	0.469955	4.346291
H	-0.465670	1.756693	3.948817
C	-4.070181	1.217325	-0.779492
H	-3.832624	2.243992	-0.487719
H	-4.608712	0.743452	0.045329
H	-4.694018	1.225993	-1.679455
C	0.697521	1.967052	-3.744819
H	1.730538	1.695115	-3.978747
H	0.711659	2.887518	-3.154483
H	0.135712	2.130088	-4.670195
C	-0.103883	-0.783449	-3.902376
H	0.922497	-1.072536	-4.143701
H	-0.640925	-0.511335	-4.816922
H	-0.593576	-1.638645	-3.431322
C	-3.100711	-1.323316	-1.688951
H	-2.247163	-1.966568	-1.915621
H	-3.724434	-1.205546	-2.581251
H	-3.678169	-1.800841	-0.892376

Geometry Optimisation for [Rh(μ-CS)Cl_2(dmpm)$_2$]

DFT: ωB97X-D/6-31G*/LANL2Dζ/gas phase

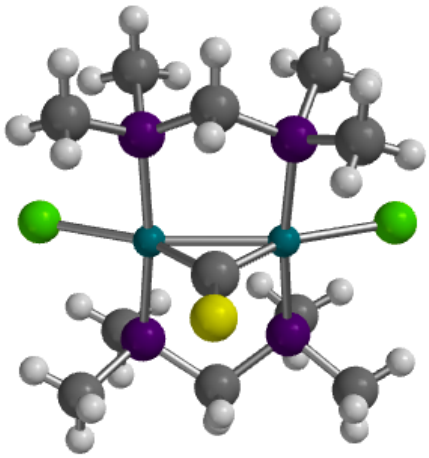

Figure S3

Table S4. Cartesian Coordinates

Atom	x	y	z
Rh	-1.119470	0.043308	0.789883
Rh	1.126735	0.177475	-0.750946
Cl	2.983059	-0.479523	-2.167921
Cl	-3.058684	-0.839788	1.955461
S	0.158561	3.044191	0.502107
P	0.041936	-0.312752	2.782197
P	-0.028330	0.610393	-2.731530
P	-2.522498	0.262728	-1.059191
P	2.517204	-0.346427	1.045638
C	-1.777949	1.137421	-2.497826
H	-1.746171	2.197794	-2.219515
H	-2.376164	1.039807	-3.410771

C	0.073859	1.458065	0.241717
Atom	**x**	**y**	**z**
C	1.839275	0.082794	2.702487
H	1.919156	1.173432	2.785770
H	2.407809	-0.367960	3.523771
C	4.143784	0.488165	1.040010
H	4.758781	0.179173	1.891544
H	3.987940	1.570153	1.071513
H	4.648687	0.241872	0.102474
C	2.943324	-2.123347	1.139596
H	3.560618	-2.350288	2.015052
H	3.487614	-2.377827	0.225819
H	2.030855	-2.723789	1.163647
C	-0.036161	-2.013082	3.452823
H	0.505334	-2.093408	4.401118
H	0.378530	-2.722603	2.733149
H	-1.090254	-2.260800	3.602659
C	-0.563414	0.722581	4.161550
H	-0.003464	0.540264	5.084547
H	-1.621426	0.494344	4.316591
H	-0.476883	1.775260	3.877540
C	-4.069415	1.193526	-0.768259
H	-3.820965	2.213894	-0.463142
H	-4.606527	0.711228	0.052444
H	-4.696791	1.219210	-1.665245
C	0.708239	1.978495	-3.694038
H	1.739251	1.705455	-3.934794
H	0.727139	2.876280	-3.069434
H	0.150218	2.178335	-4.614580
C	-0.112203	-0.768286	-3.931888
H	0.913451	-1.056760	-4.176086
H	-0.644627	-0.472412	-4.841753
H	-0.608420	-1.630722	-3.481306
C	-3.106257	-1.343349	-1.713083
H	-2.251959	-1.981804	-1.950375
H	-3.735217	-1.219593	-2.600805
H	-3.678109	-1.831124	-0.918619

Geometry Optimisation for [Rh(μ-CSe)Cl_2(dmpm)$_2$]

DFT: ωB97X-D/6-31G*/LANL2Dζ/gas phase

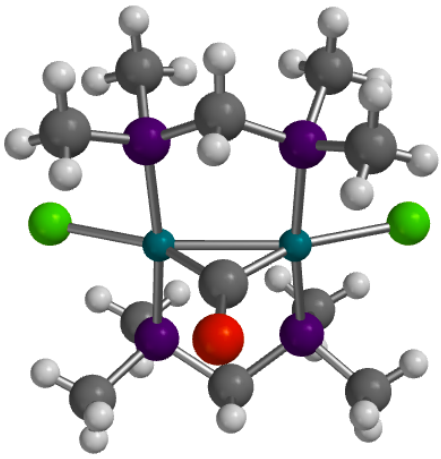

Figure S4

Table S5. Cartesian Coordinates

Atom	**x**	**y**	**z**
Rh	-1.118403	0.017032	0.776626
Rh	1.135207	0.174669	-0.745656
Cl	2.996606	-0.458311	-2.167898
Cl	-3.062959	-0.867223	1.931479
Se	0.138809	3.162245	0.522199
P	0.038837	-0.348597	2.771961
P	-0.022591	0.580876	-2.732907
P	-2.528583	0.272661	-1.065130
P	2.529939	-0.327456	1.055565
C	-1.766894	1.125041	-2.507447
H	-1.722861	2.187070	-2.237274
H	-2.363964	1.027257	-3.421105
C	0.065845	1.430544	0.239765
C	1.829406	0.075674	2.708663
H	1.889077	1.166908	2.800841
H	2.400265	-0.370993	3.530494
C	4.130459	0.553699	1.056239
H	4.752257	0.261328	1.908642
H	3.942072	1.630537	1.089184
H	4.644740	0.324268	0.119429
C	2.999409	-2.093167	1.142997
H	3.624618	-2.306035	2.016213
H	3.546499	-2.332723	0.226936
H	2.101743	-2.715588	1.169360
C	-0.022378	-2.056665	3.423744
H	0.512400	-2.140041	4.375550
H	0.406935	-2.753485	2.700231
H	-1.074541	-2.318742	3.562883
C	-0.591109	0.667535	4.154030
H	-0.032603	0.488950	5.078625
H	-1.646133	0.421761	4.301700
H	-0.519357	1.722743	3.874937
C	-4.027684	1.265738	-0.740154

H	-3.727129	2.268172	-0.422311
H	-4.575134	0.795529	0.080788
H	-4.665920	1.335041	-1.627033
C	0.717612	1.925350	-3.725201
H	1.746395	1.643776	-3.964946
H	0.742285	2.834778	-3.117787
H	0.155712	2.109243	-4.646697
C	-0.112179	-0.825677	-3.899387
H	0.912273	-1.119155	-4.143216
H	-0.650165	-0.553264	-4.813298
H	-0.604157	-1.677662	-3.424677
C	-3.183597	-1.304952	-1.720500
H	-2.359228	-1.969830	-1.989010
H	-3.829783	-1.146518	-2.590005
H	-3.752047	-1.782342	-0.917445

Geometry Optimisation for [Rh(μ-CSe)(μ-HCCH)Cl_2(dHpm)$_2$]

DFT: ωB97X-D/6-31G*/LANL2Dζ/gas phase

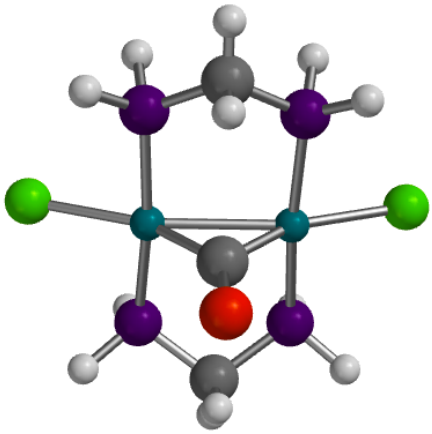

Figure S5

Table S6. Cartesian Coordinates

Atom	x	y	z
Rh	-1.139046	-0.194105	0.741387
Rh	1.127726	-0.042638	-0.781438
Cl	2.977772	-0.663131	-2.168140
Cl	-3.056844	-1.067506	1.877852
Se	0.138858	2.944185	0.496294
P	0.038884	-0.697636	2.678308
P	-0.062013	0.219082	-2.758435
P	-2.525118	0.015208	-1.111287
P	2.496793	-0.584358	1.013926
C	-1.787819	0.851666	-2.583175
H	-1.707751	1.914699	-2.330682
H	-2.386391	0.746579	-3.490633
C	0.056426	1.227850	0.207710
C	1.820439	-0.211597	2.690818
H	1.847927	0.877692	2.803776
H	2.390973	-0.667069	3.503175
H	-3.755033	0.675668	-0.956037
H	-2.978912	-1.202079	-1.648960
H	0.476501	1.045982	-3.758279
H	-0.241473	-0.960040	-3.502196
H	3.786694	-0.030605	1.061944
H	2.823617	-1.948236	1.114312
H	-0.433945	-0.185356	3.897654
H	0.091735	-2.064256	3.002108

Geometry Optimisation for [Rh(μ-CSe)$Cl_2$$(CO)_6$]

DFT: ωB97X-D/6-31G*/LANL2Dζ/gas phase

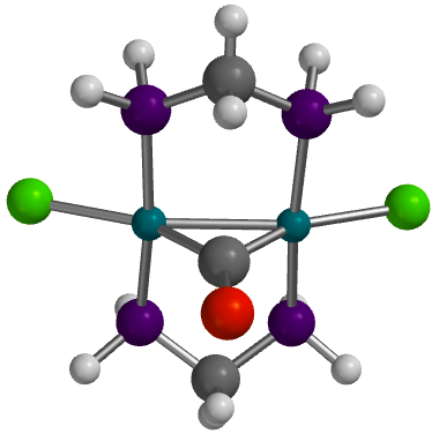

Figure S6

Table S7. Cartesian Coordinates

Atom	x	y	z
Rh	0.237287	1.342368	-0.139697
Rh	-0.181075	-1.357964	0.034697
C	-1.371515	1.665285	-1.187074
O	-2.267191	1.923630	-1.834374
C	-0.541679	2.256741	1.541582
O	-0.988900	2.702694	2.485236
C	2.028728	1.248037	0.612738
O	3.093721	1.265207	1.004684
C	1.572112	-1.719633	0.796067
O	2.591090	-2.010748	1.202269
C	-1.835881	-1.303405	-0.988290
O	-2.782649	-1.354374	-1.612038
C	-1.159995	-1.779161	1.804493
O	-1.698144	-1.949477	2.789765
Cl	0.007814	-3.644819	-0.857999
Cl	1.094990	3.337021	-1.301865
C	0.721284	-0.203712	-1.420079
Se	1.480001	-0.417689	-2.930114

Geometry Optimisation for [Rh(μ-CSe)Cl_2($CO)_4$]

DFT: ωB97X-D/6-31G*/LANL2Dζ/gas phase

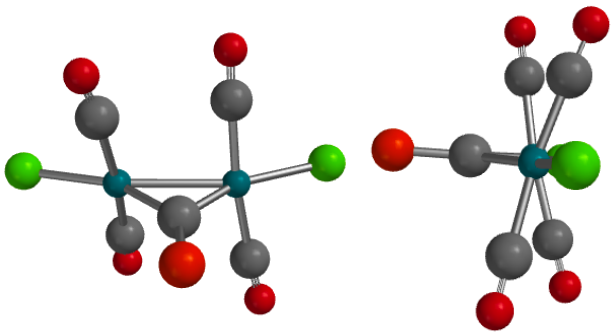

Figure S7

Table S8. Cartesian Coordinates

Atom	x	y	z
Rh	0.055153	1.384068	-0.028586
Rh	-0.168823	-1.350386	0.258565
C	-1.429050	1.784151	-1.256251
O	-2.277005	2.077273	-1.949105
C	1.431018	1.252944	1.347507
O	2.212990	1.225609	2.169257
C	1.643514	-1.844964	0.837645
O	2.664884	-2.188058	1.190143
C	-2.069093	-1.068474	-0.087550
O	-3.184857	-0.944572	-0.251915
C	0.573806	-0.165259	-1.130220
Se	1.333460	-0.387206	-2.641312
Cl	-0.790122	-3.465368	1.089204
Cl	0.004125	3.690243	0.452618

Geometry Optimisation for [Rh(μ-CSe)Cl_2(μ-HCCH)($dmpm)_2$]

DFT: ωB97X-D/6-31G*/LANL2Dζ/gas phase

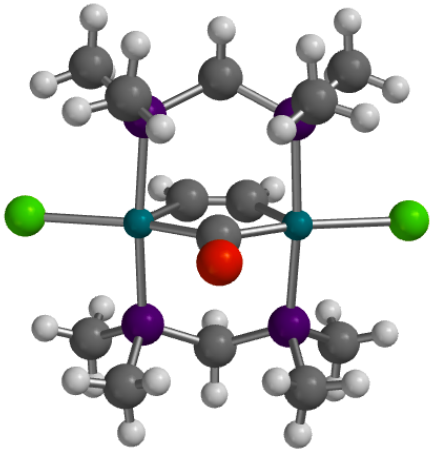

Figure S8

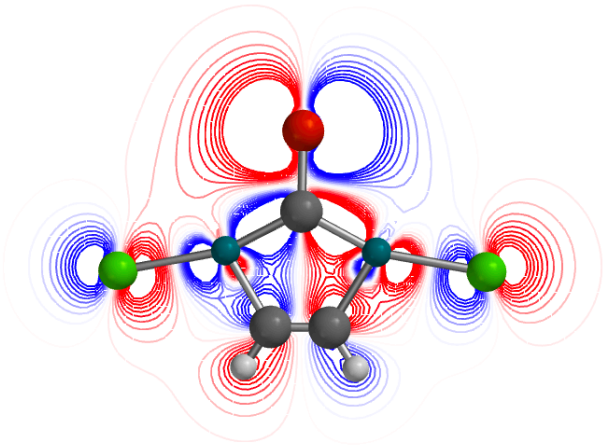

Figure S9. Slice of the HOMO through the equatorial coordination plane (dmpm ligands omitted for clarity).

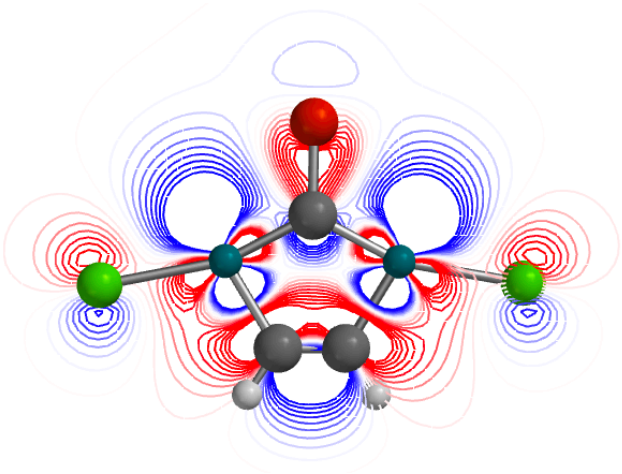

Figure S10. Slice of the LUMO through the equatorial coordination plane (dmpm ligands omitted for clarity).

Table S11. Cartesian Coordinates

Atom	x	y	z
Rh	-0.319062	1.383500	-0.938768
Rh	0.542619	-1.434625	0.761966
Se	2.189171	-0.393911	-1.793352
Cl	-1.257217	3.480292	-1.905229
Cl	0.795963	-3.388058	2.281872
P	1.004666	2.591357	0.581821
P	-0.938929	-2.608009	-0.634810
P	1.832780	-0.065223	2.174202
P	-1.764016	0.047967	-2.225866
C	1.389406	1.730880	2.174236
H	2.166176	2.292520	2.707411
H	0.467957	1.795270	2.761444
C	0.801591	-0.152773	-0.651962
C	-1.027726	-0.332775	1.312546
C	-1.365538	0.768601	0.647899
H	-2.219157	1.394791	0.922845
H	-1.573954	-0.701992	2.185000
C	2.624132	3.113552	-0.084597
H	3.164298	2.240462	-0.460247
H	3.224477	3.631892	0.669755
H	2.439495	3.784399	-0.928693
C	0.243698	4.138018	1.181090
H	0.910730	4.681588	1.857463
H	-0.689752	3.896552	1.696966
H	-0.007599	4.750136	0.311002
C	3.625092	-0.113993	1.819997
H	4.183032	0.578516	2.458158
H	3.797057	0.123281	0.766651
H	3.976671	-1.134894	1.995785
C	1.716197	-0.467411	3.951009
H	2.354146	0.185326	4.555452
H	2.002408	-1.514037	4.080653
H	0.675392	-0.368608	4.271133
C	-0.114276	-3.539810	-1.973065
H	0.524292	-4.299753	-1.513291
H	0.527645	-2.865733	-2.546805
H	-0.838885	-4.024973	-2.634521
C	-1.967370	-3.854930	0.212579
H	-1.300574	-4.553797	0.723819
H	-2.618418	-4.386368	-0.488707
H	-2.572311	-3.358740	0.976438
C	-3.407419	0.784312	-2.525401
H	-3.261174	1.755293	-3.005207
H	-3.896256	0.960210	-1.563223
H	-4.034212	0.136860	-3.146779
C	-1.129742	-0.344225	-3.893744
H	-0.145028	-0.811908	-3.809190
H	-1.009670	0.597090	-4.437969
H	-1.811332	-1.000488	-4.444228
C	-2.223041	-1.583617	-1.484426
H	-2.729018	-2.194980	-2.241490
H	-2.957415	-1.347036	-0.707624

Figure S11. Variation of the HOMO energy and topology for the series [$Rh_2(\mu$-CA)Cl_2(dmpm)$_2$] (A = O, S, Se; DFT: ωB97X-D/6-31G*/LANL2Dζ, gas phase))

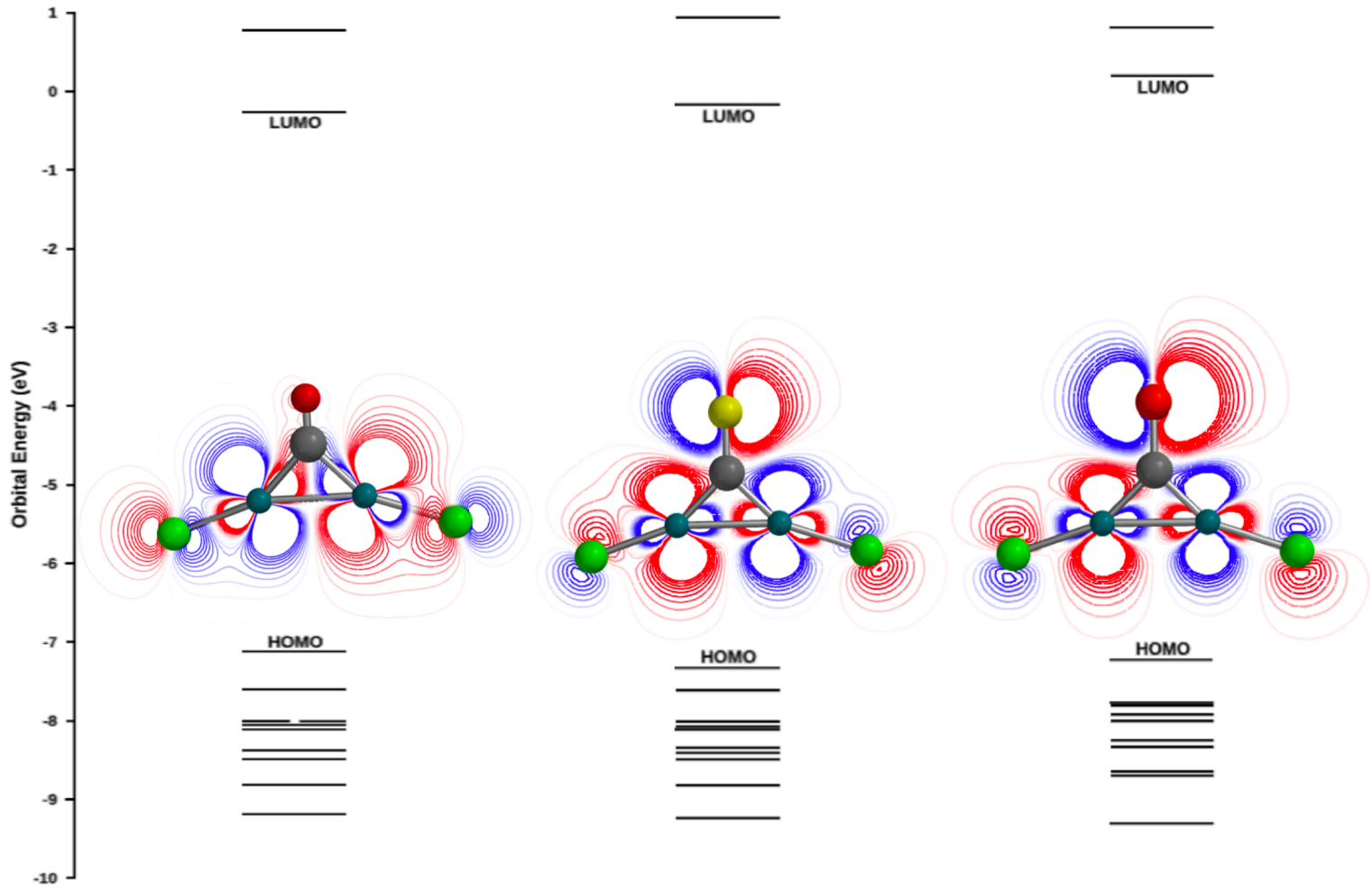

Figure S12. Time-lapse $^{31}P\{^{1}H\}$ NMR Spectra of the Reaction of $[Ru(\mu\text{-}C)Cl_2(\mu\text{-dppm})_2]$ with CS_2.

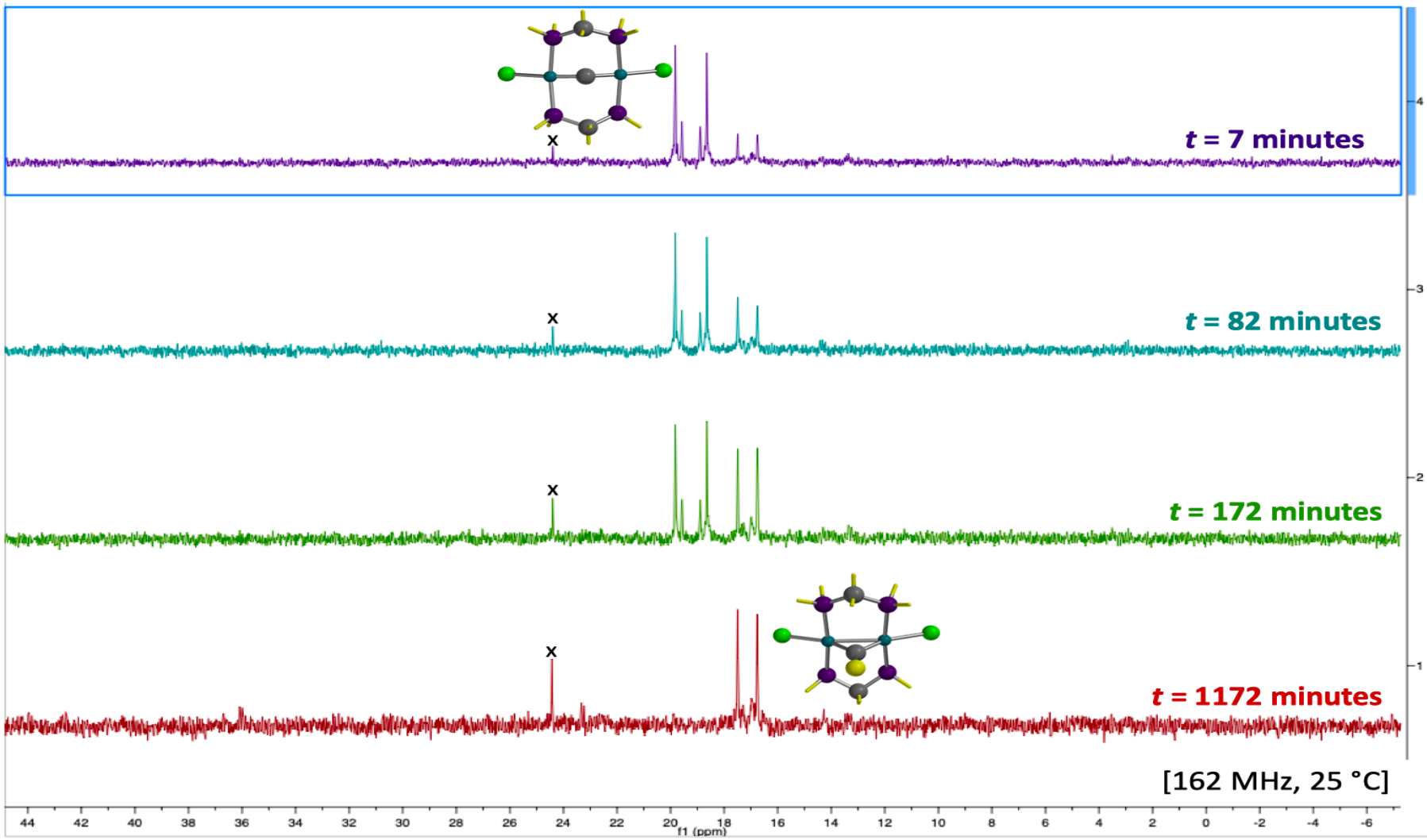

Figure S13. ^{1}H NMR Spectrum of [$Rh_2(\mu$-CS)$Cl_2(dppm)_2$] (4) 600 MHz, 25 °C, $CDCl_3$

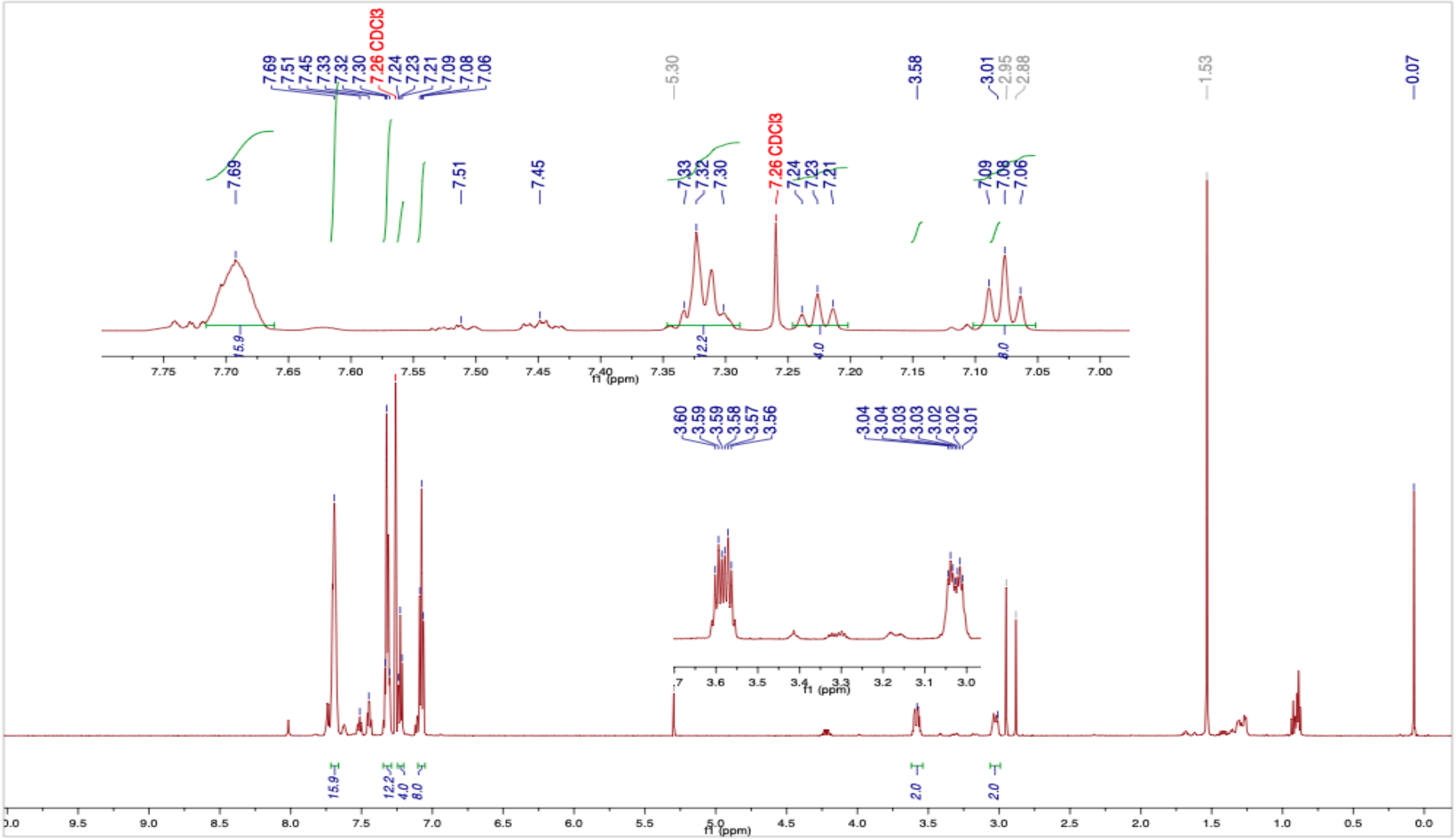

Figure S14. $^{31}P\{^{1}H\}$ NMR Spectrum of $[Rh_2(\mu\text{-}CS)Cl_2(dppm)_2]$ (4) 162 MHz, 25 °C, $CDCl_3$

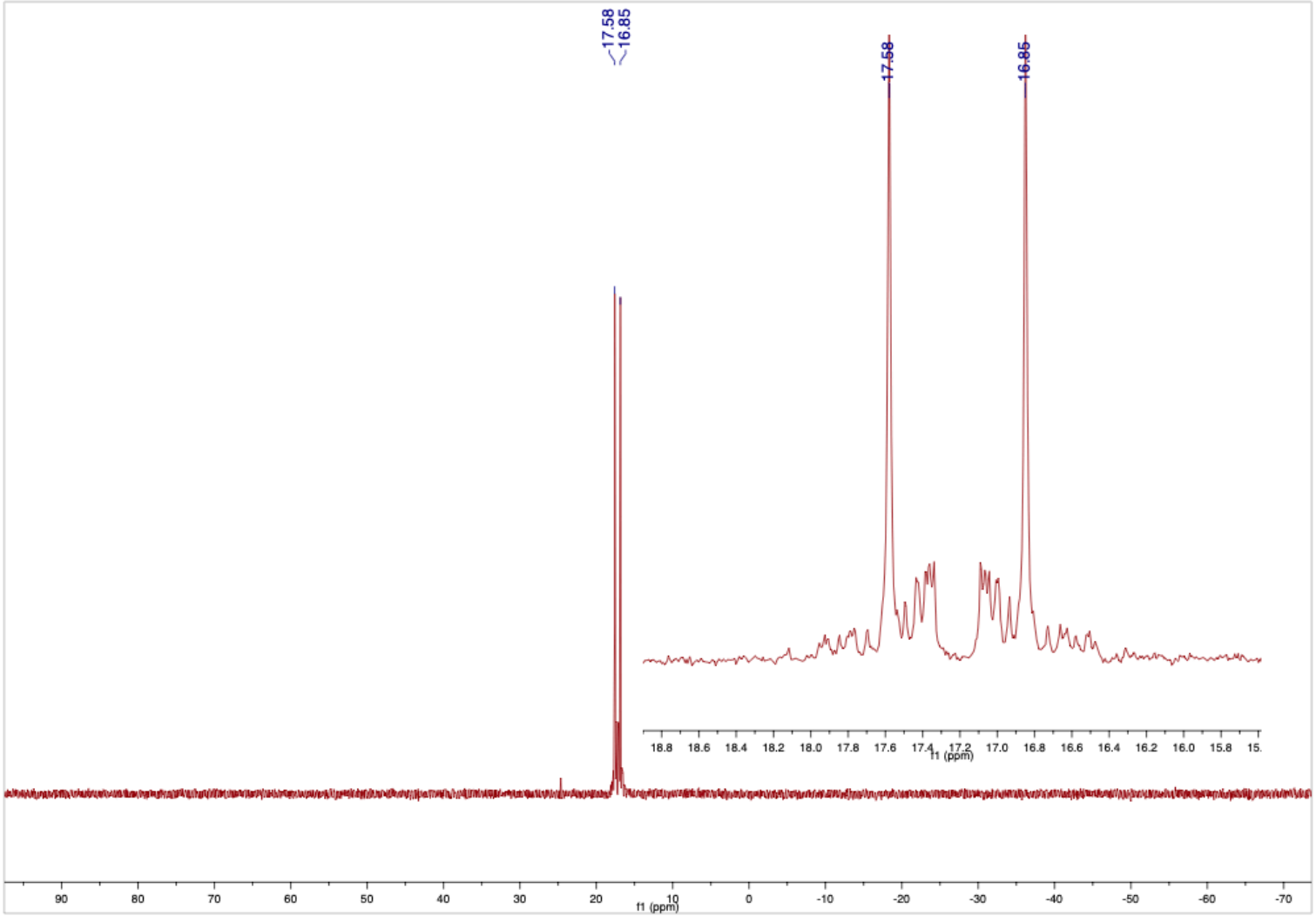

Figure S15. $^{13}C\{^{1}H\}$ NMR Spectrum of $[Rh_2(\mu\text{-}CS)Cl_2(dppm)_2]$ (4) 151 MHz, 25 °C, $CDCl_3$

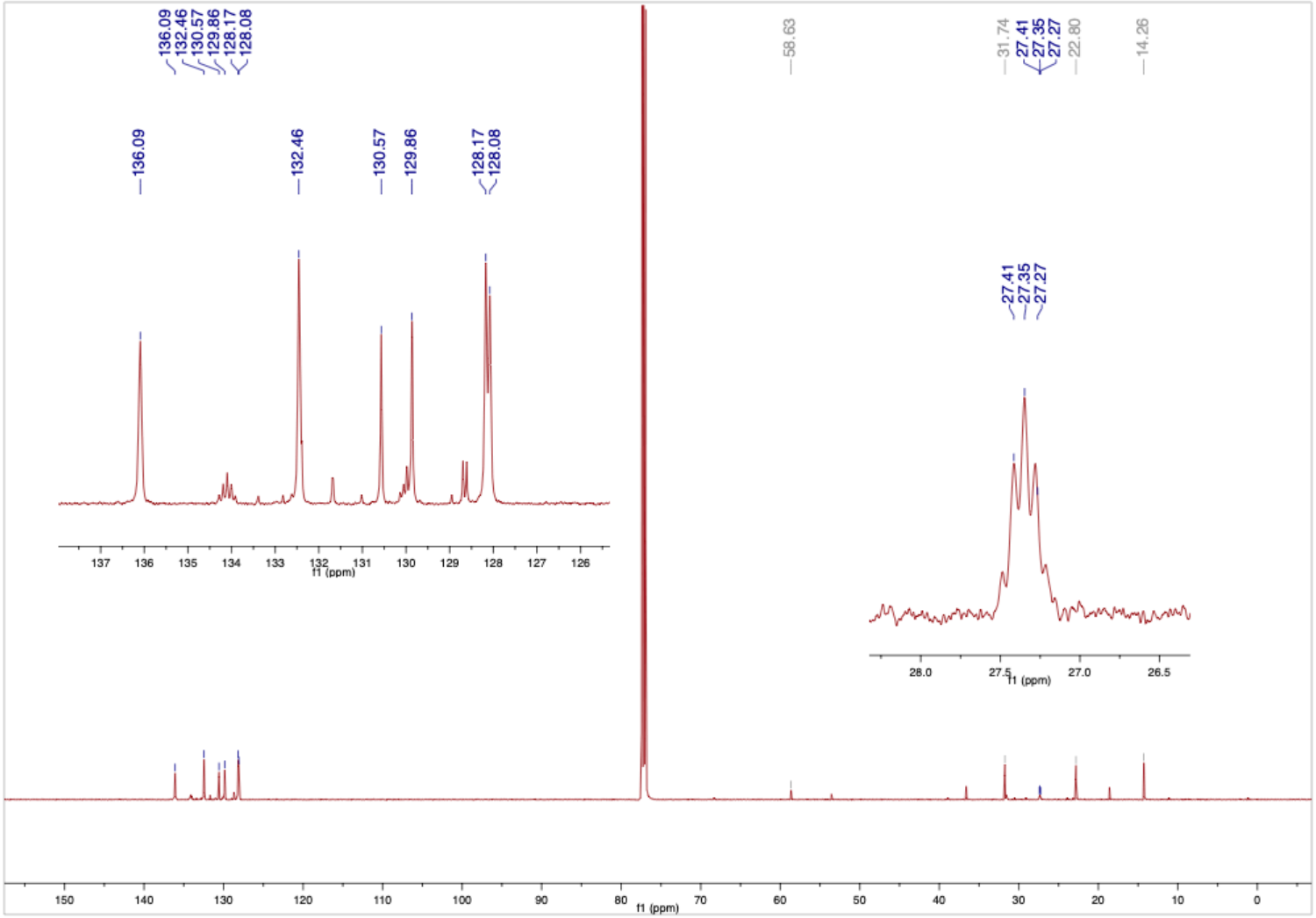

Figure 16. COSY ^{1}H NMR Spectrum of $[Rh_2(\mu\text{-}CS)Cl_2(dppm)_2]$ (4) 600 MHz, 25 °C, $CDCl_3$

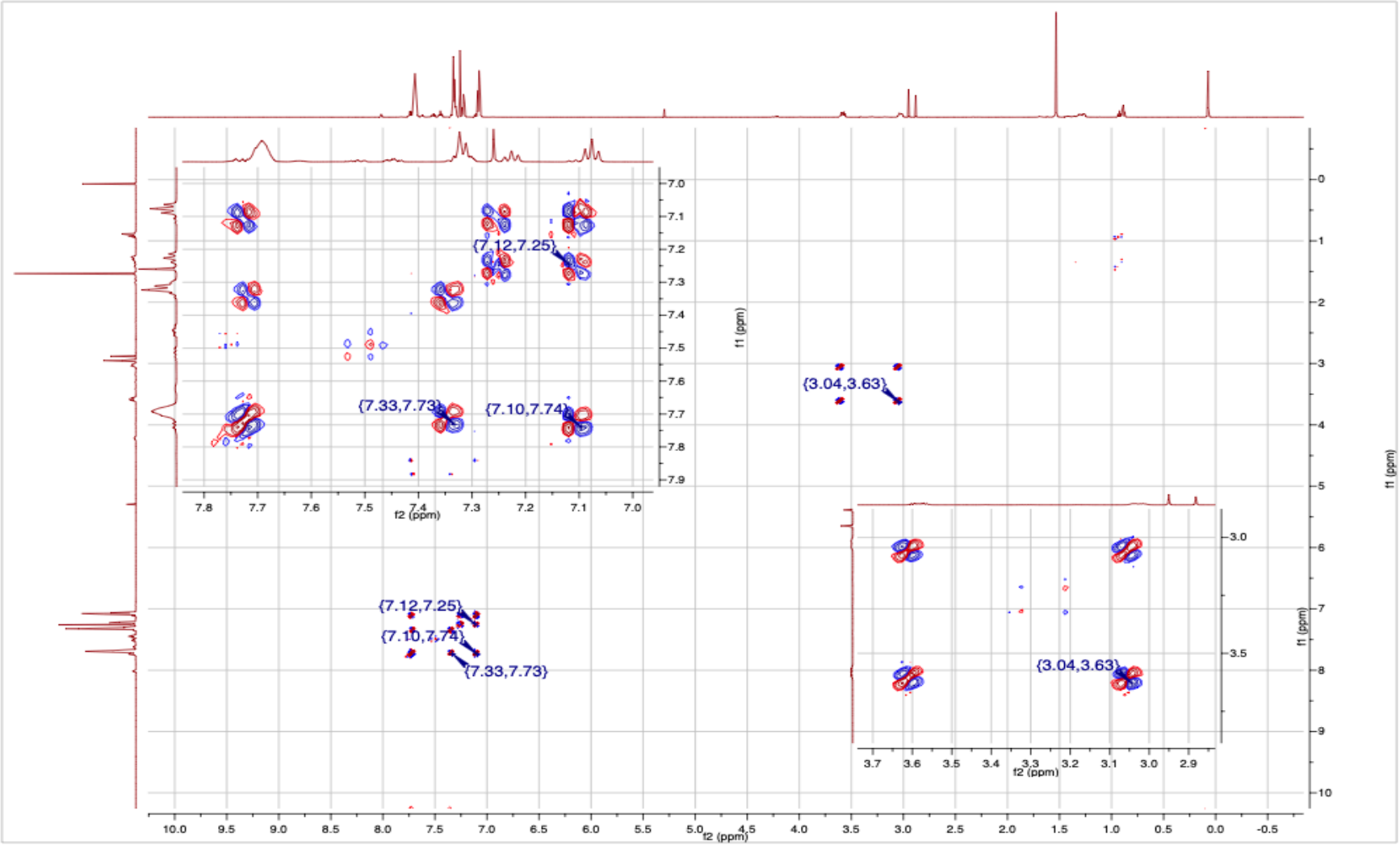

Figure 17. HSQC ^{1}H(600 MHz)-^{13}C(151 MHz) NMR Spectrum of $[Rh_2(\mu\text{-}CS)Cl_2(dppm)_2]$ (4) 600 MHz, 25 °C, $CDCl_3$

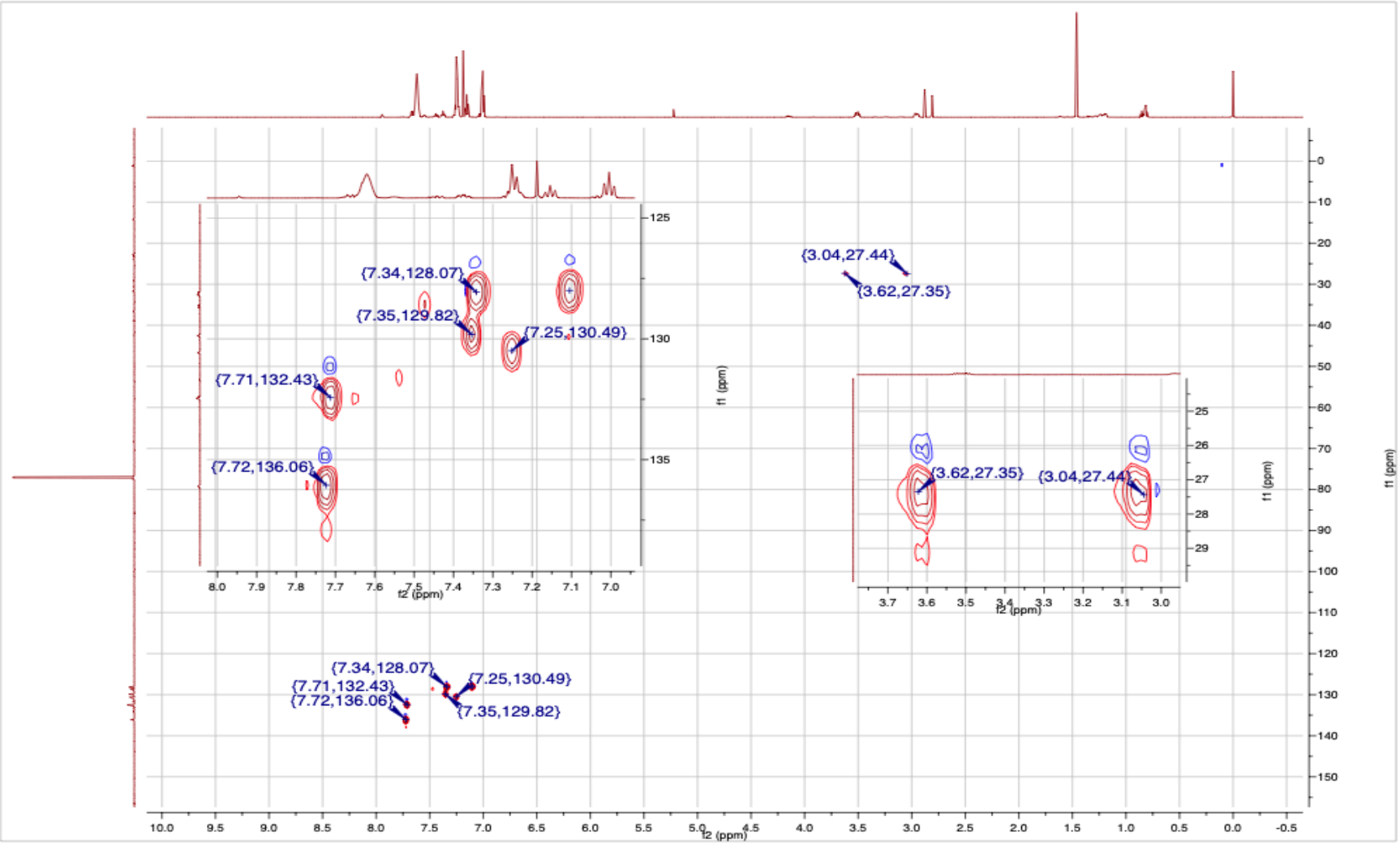

Figure S18. ATR-FT-IR of [$Rh_2(\mu$-CS)Cl_2(dppm)$_2$] (4)

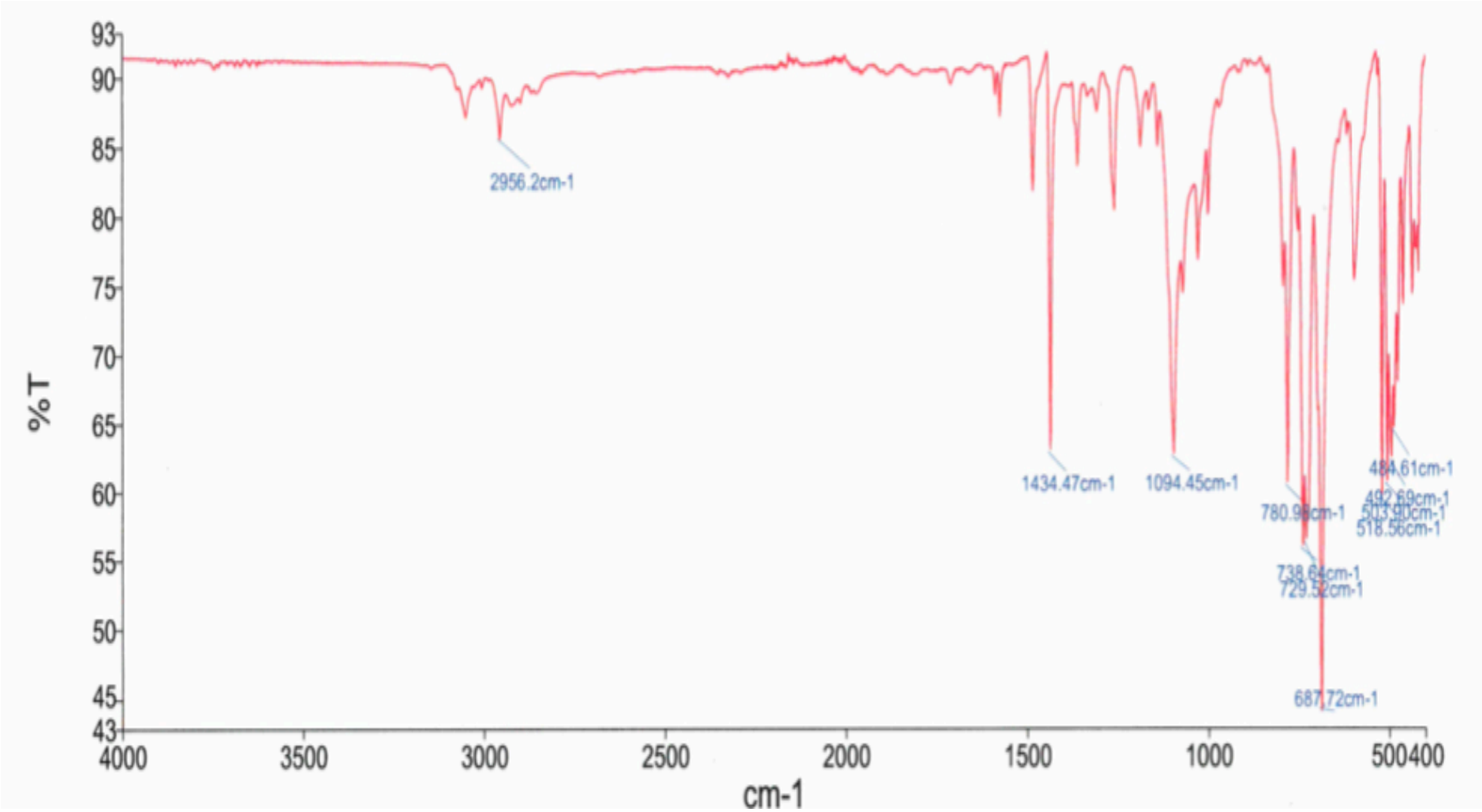

Figure S19. ESI-Mass Spectrum of of [$Rh_2(\mu$-CS)Cl_2(dppm)$_2$] (4)

Single Mass Analysis
Tolerance = 3.0 PPM / DBE: min = -1.5, max = 35.0
Element prediction: Off
Number of isotope peaks used for i-FIT = 3

Monoisotopic Mass, Even Electron Ions
560 formula(e) evaluated with 1 results within limits (up to 50 best isotopic matches for each mass)
Elements Used:
C: 0-60 H: 0-60 O: 0-4 P: 0-4 S: 0-1 35Cl: 0-1 37Cl: 0-1 103Rh: 0-2
HB-1234-1/AJ
0065 32 (0.138) Cm (29:40)

1: TOF MS ES+
4.66e+005

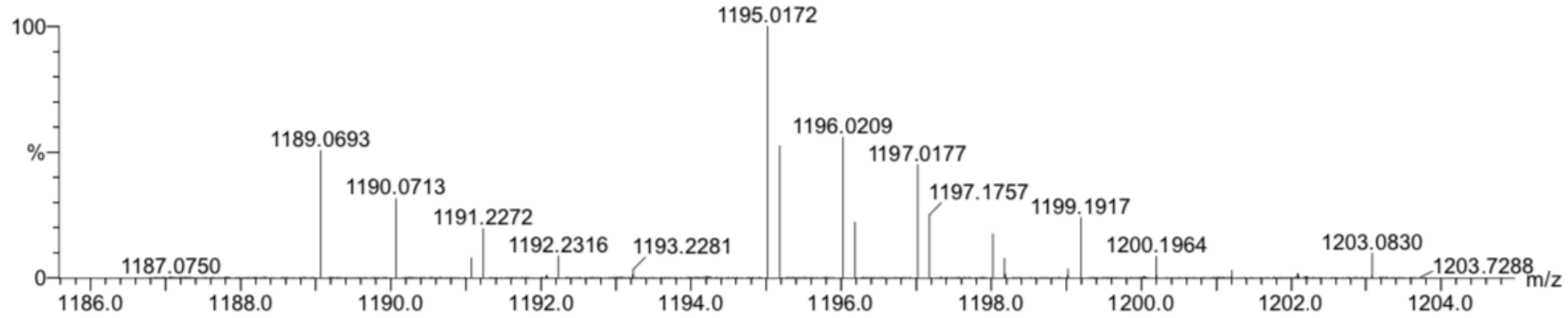

Minimum:				-1.5				
Maximum:		5.0	3.0	35.0				
Mass	Calc. Mass	mDa	PPM	DBE	i-FIT	Norm	Conf(%)	Formula
1195.0172	1195.0179	-0.7	-0.6	34.5	790.5	n/a	n/a	C57 H50 O4 P4 S 35Cl 103Rh2

Figure S20. ^{1}H NMR Spectrum of [Rh_2(μ-CSe)Cl_2(μ-dppm)$_2$] (5) – 600 MHz, 25 °C, $CDCl_3$

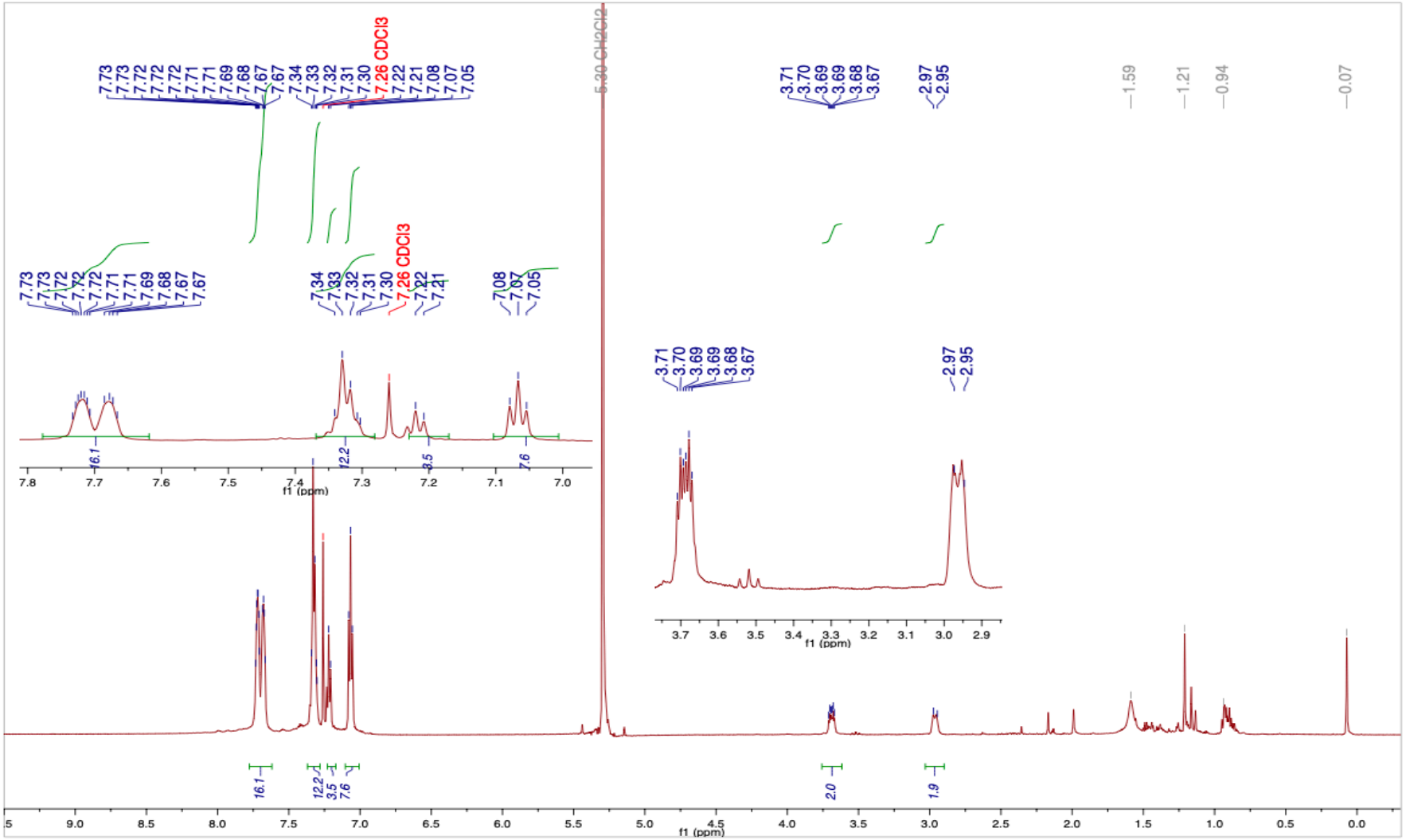

Figure S21. $^{31}P\{^{1}H\}$ **NMR Spectrum of** $[Rh_2(\mu\text{-}CSe)Cl_2(\mu\text{-}dppm)_2]$ **(5) 162 MHz, 25 °C,** $CDCl_3$

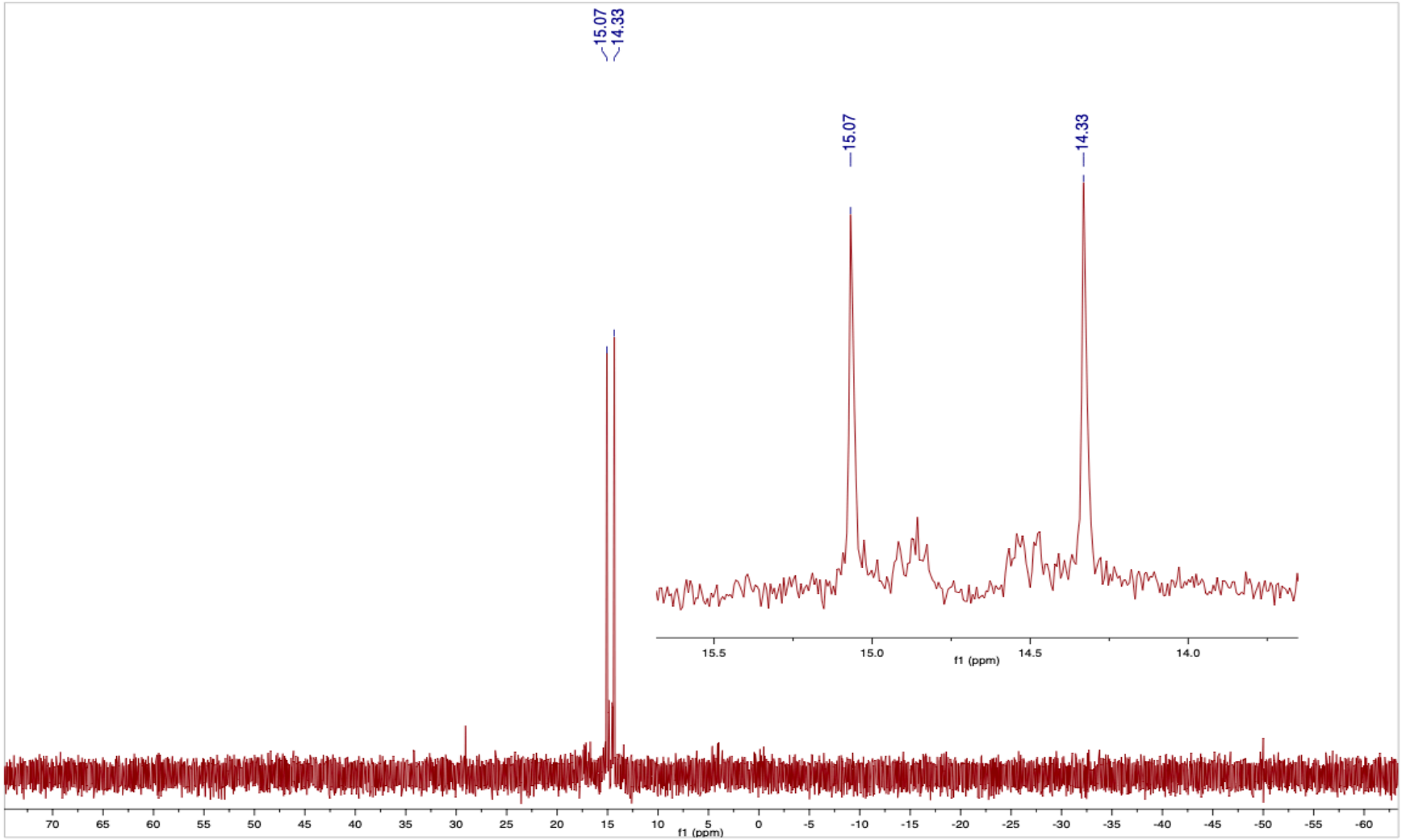

Figure S22. $^{13}C\{^{1}H\}$ **NMR Spectrum of** $[Rh_2(\mu\text{-}CSe)Cl_2(\mu\text{-}dppm)_2]$ **(5) 151 MHz, 25 °C,** $CDCl_3$

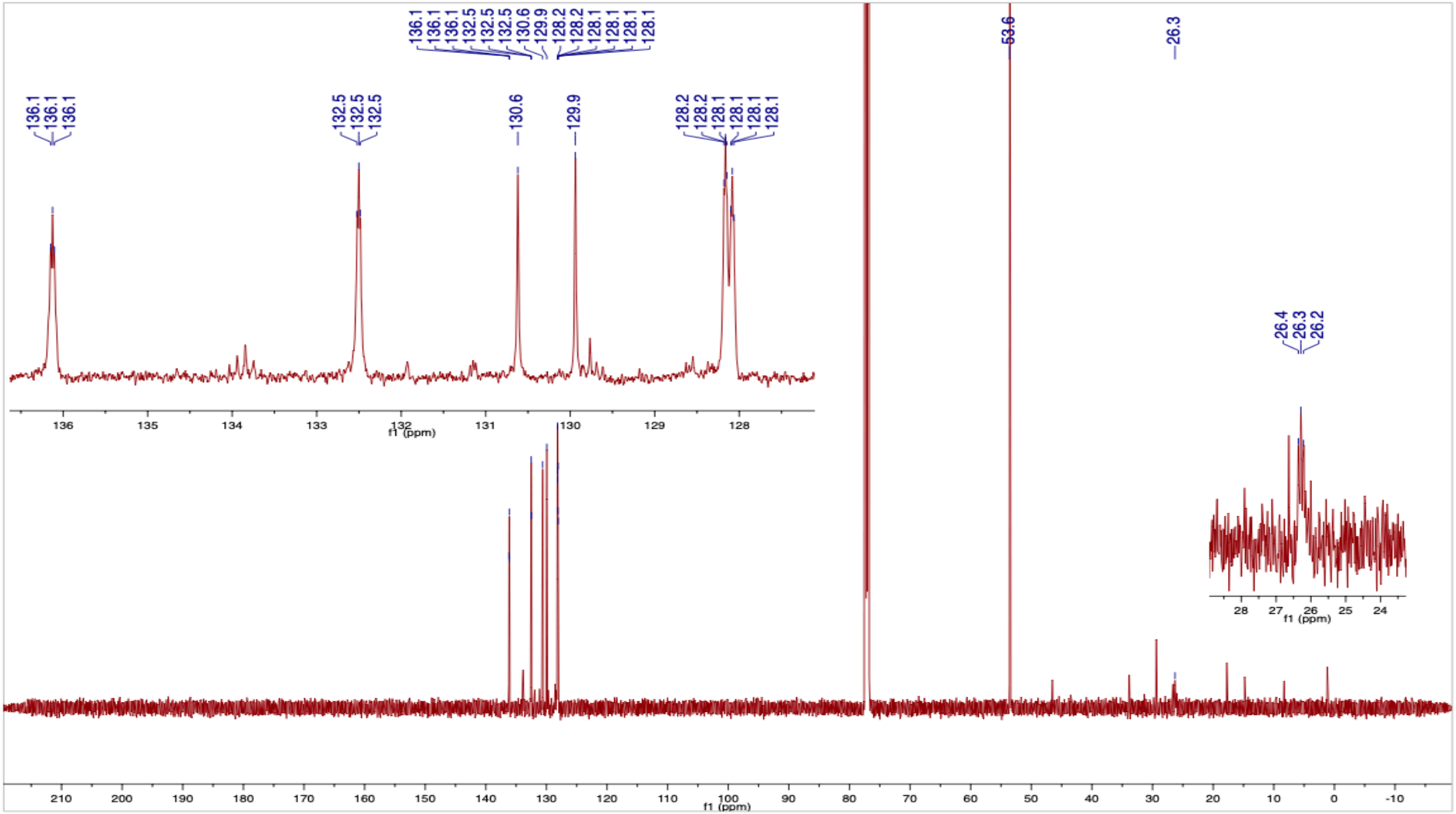

Figure S23. Wide sweep-width $^{13}C\{^1H\}$ NMR spectrum of $[Rh_2(\mu\text{-CSe})Cl_2(\mu\text{-dppm})_2]$ (5) 50-460 ppm, 101 MHz, 25 °C, $CDCl_3$. [δ(CSe) resonance not located]

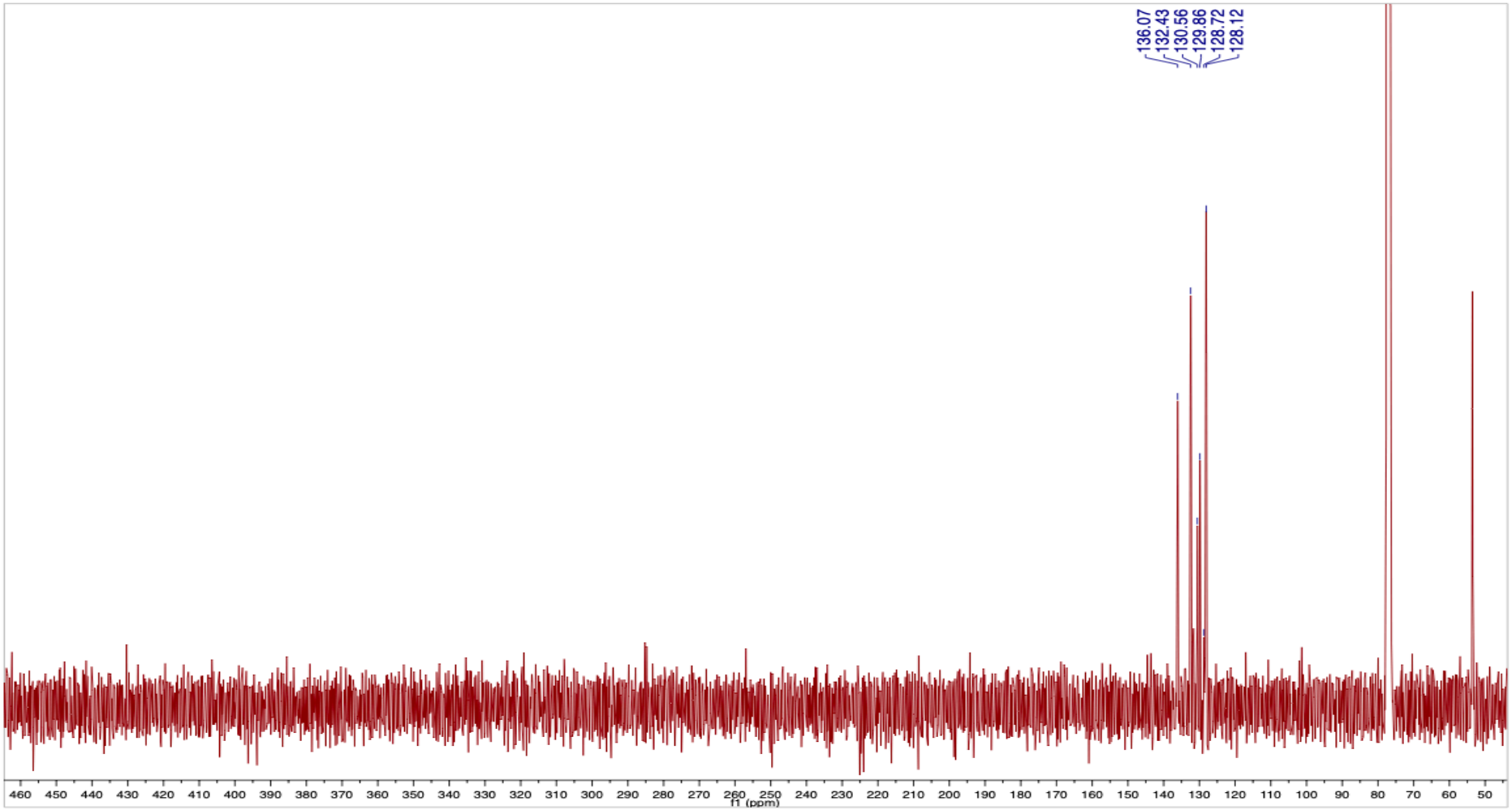

Figure S24. $^{77}Se\{^{1}H\}$ NMR Spectrum of $[Rh_2(\mu\text{-CSe})Cl_2(\mu\text{-dppm})_2]$ (5) – 133.6 MHz, 25 °C, $CDCl_3$, 25671 scans, δ(CSe) resonance not located

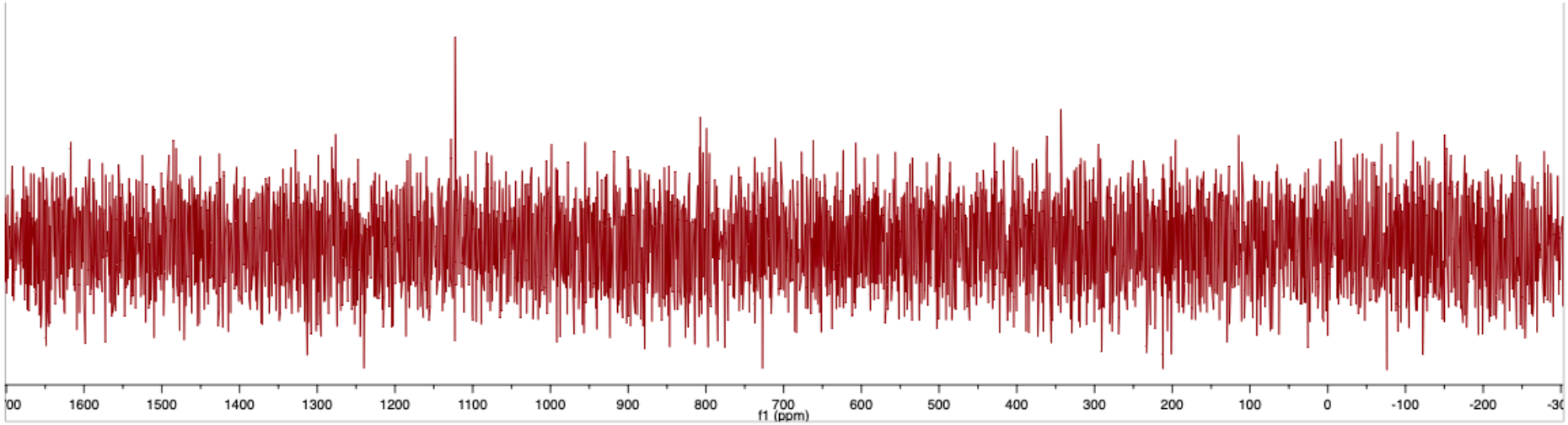

Figure S25. ^{13}C(151 MHz)-^{1}H(600 MHz)-HMBC NMR Spectrum of $[Rh_2(\mu\text{-}CSe)Cl_2(\mu\text{-}dppm)_2]$ (5), 25 °C, $CDCl_3$.

Figure S26. HSQC ^{13}C(151 MHz)-^{1}H(600 MHz) NMR Spectrum of $[Rh_2(\mu\text{-}CSe)Cl_2(\mu\text{-}dppm)_2]$ (5), 25 °C, $CDCl_3$.

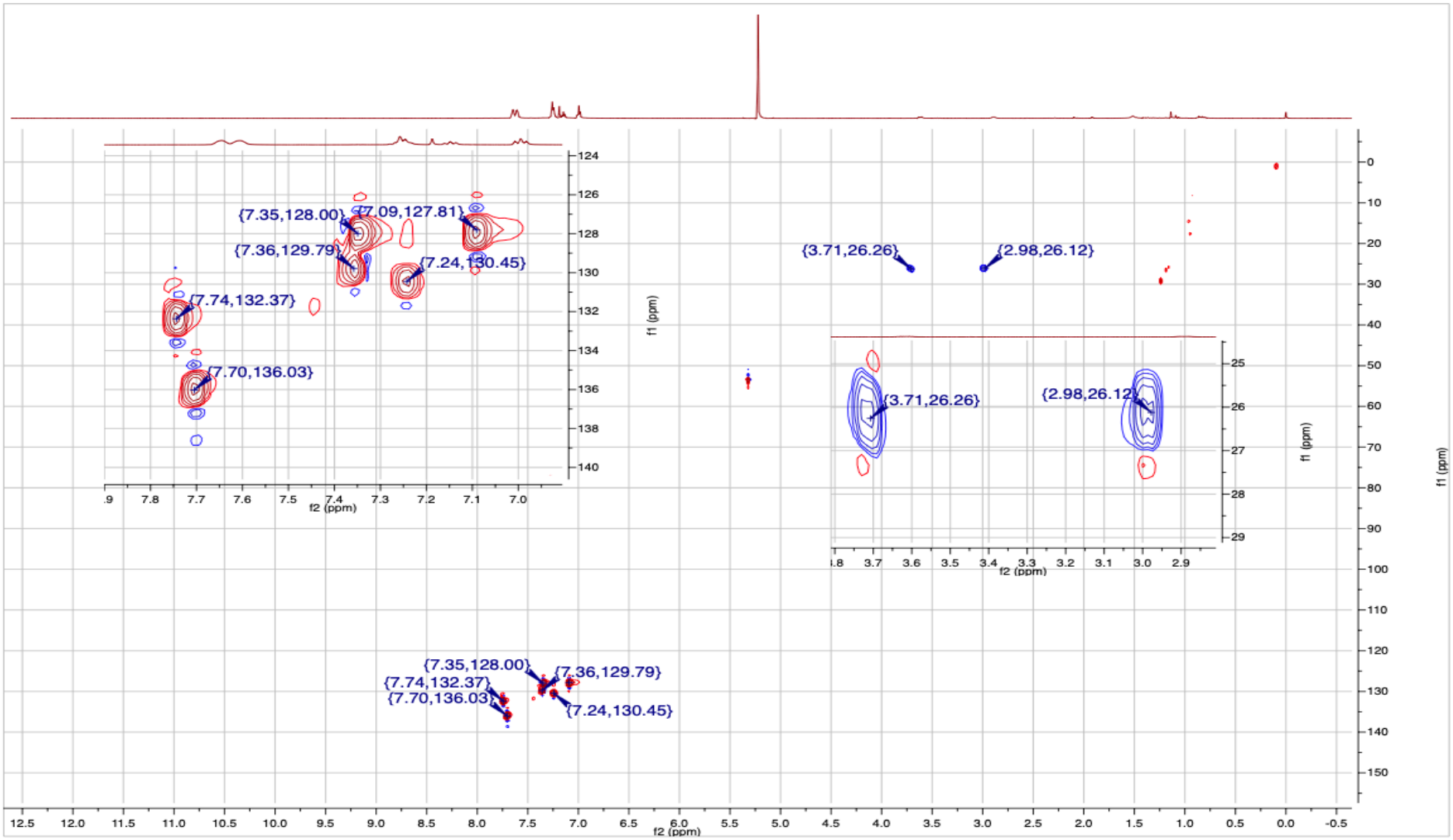

Figure S27. COSY ^{1}H(600 MHz) NMR Spectrum of [Rh_2(μ-CSe)Cl_2(μ-dppm)$_2$] (5), 25 °C, $CDCl_3$.

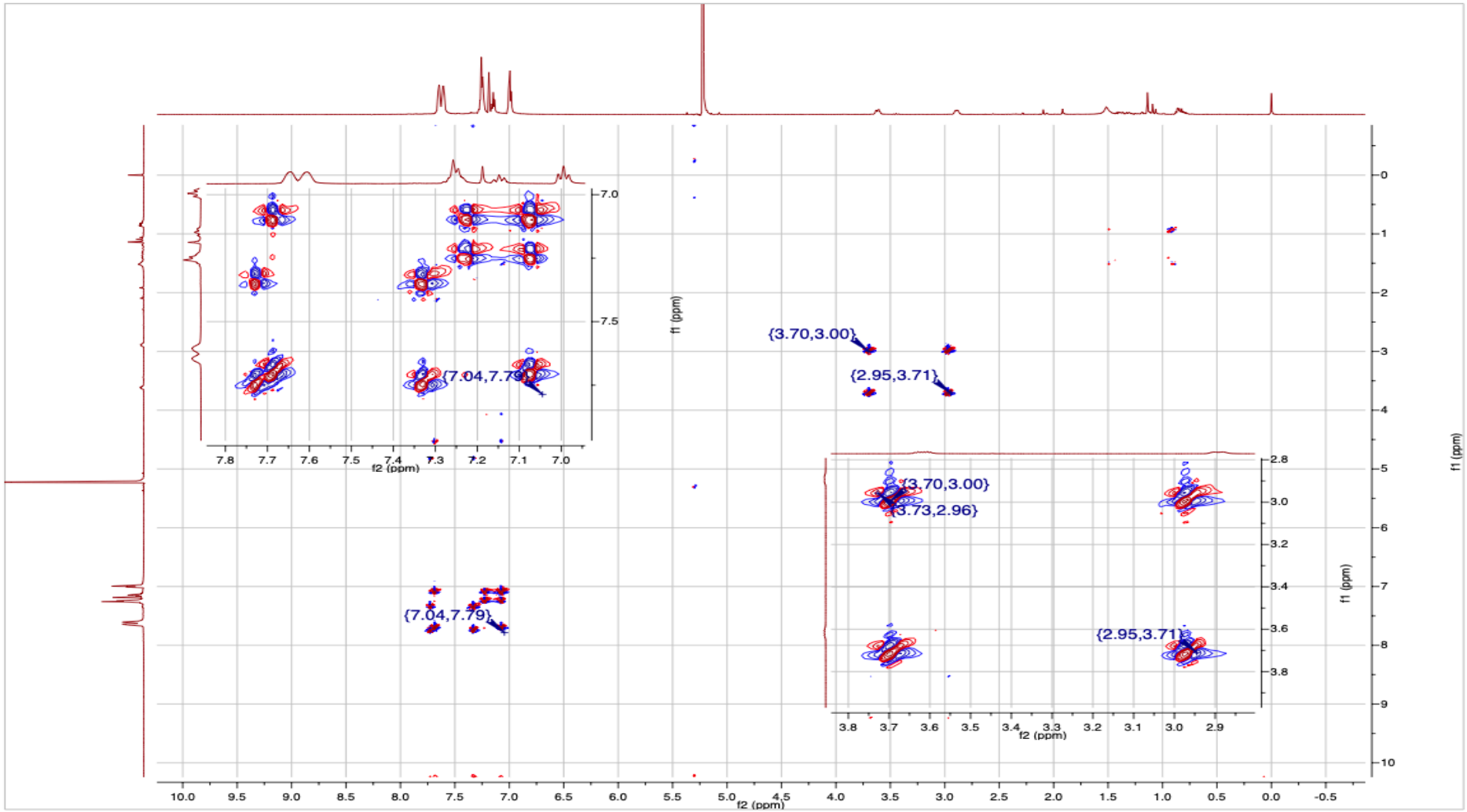

Figure S28. ATR-FT-IR spectrum of [Rh_2(μ-CSe)Cl_2(μ-dppm)$_2$] (5)

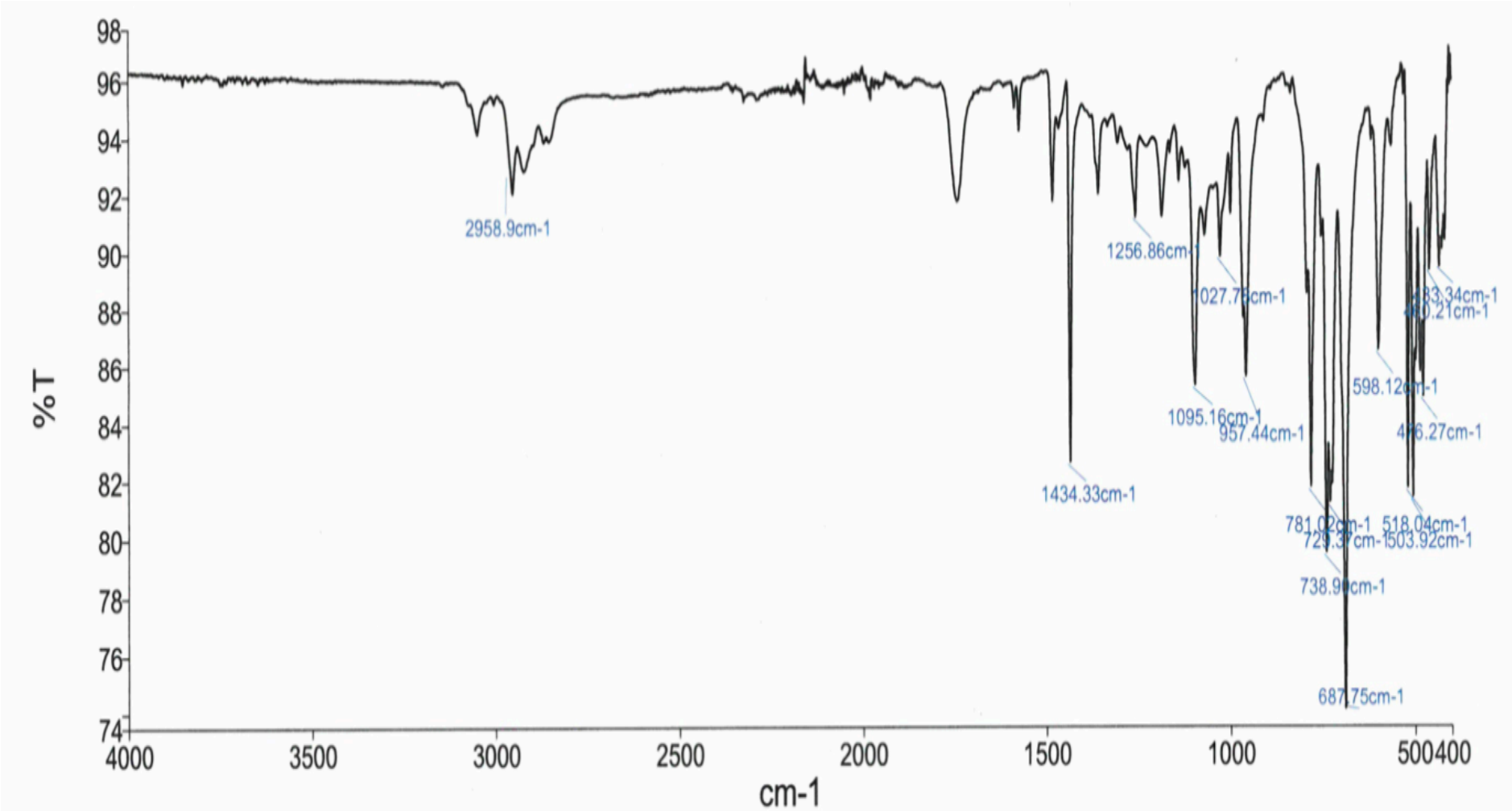

Figure S29. ATR-FT-IR Difference Spectrum of $[Rh_2(\mu\text{-}CS)Cl_2(\mu\text{-}dppm)_2]$ (4) – $[Rh_2(\mu\text{-}CSe)Cl_2(\mu\text{-}dppm)_2]$ (5)

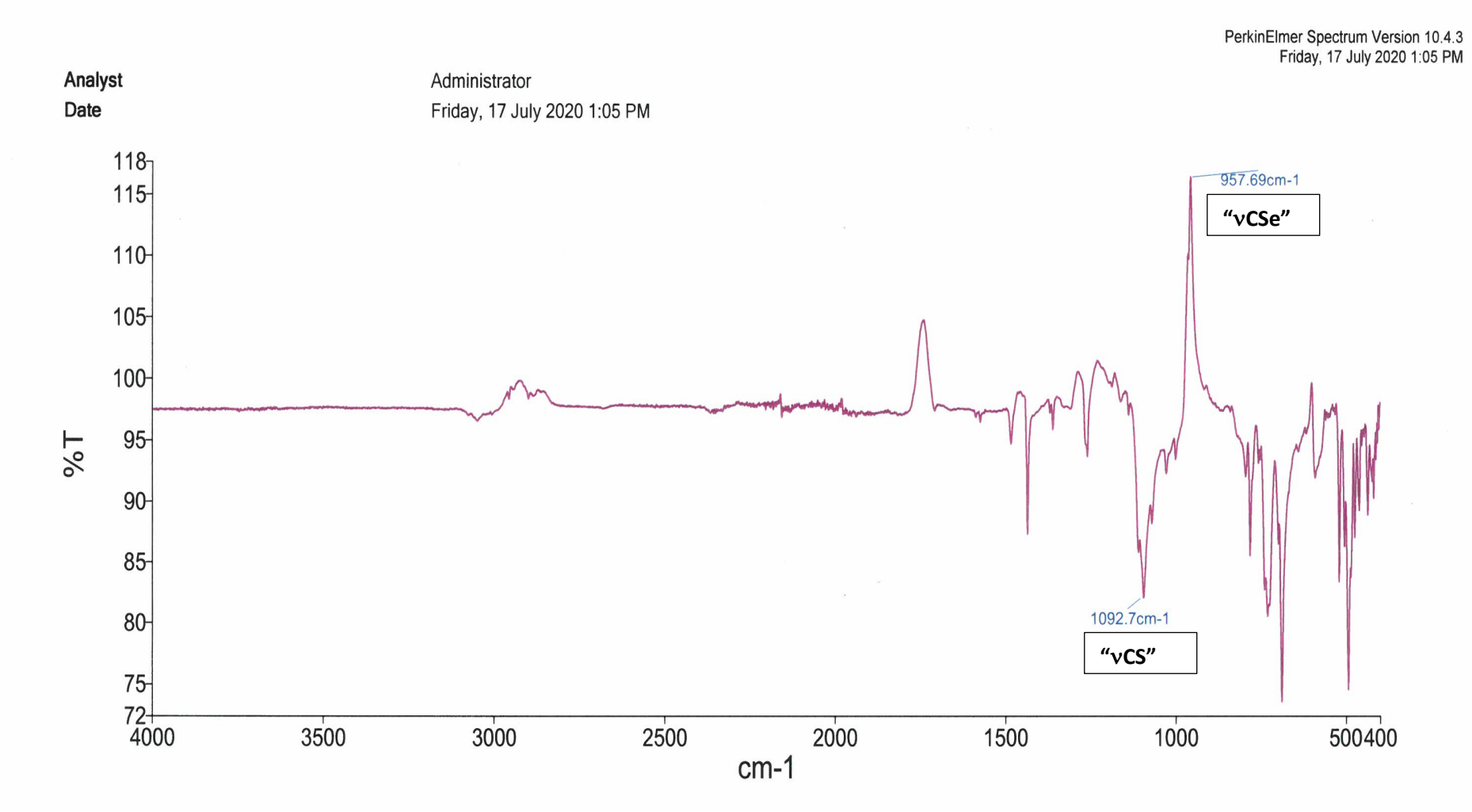

Figure S30. ESI-MS (Accurate Mass) Spectrum of $[Rh_2(\mu\text{-CSe})Cl_2(\mu\text{-dppm})_2]$ (5)

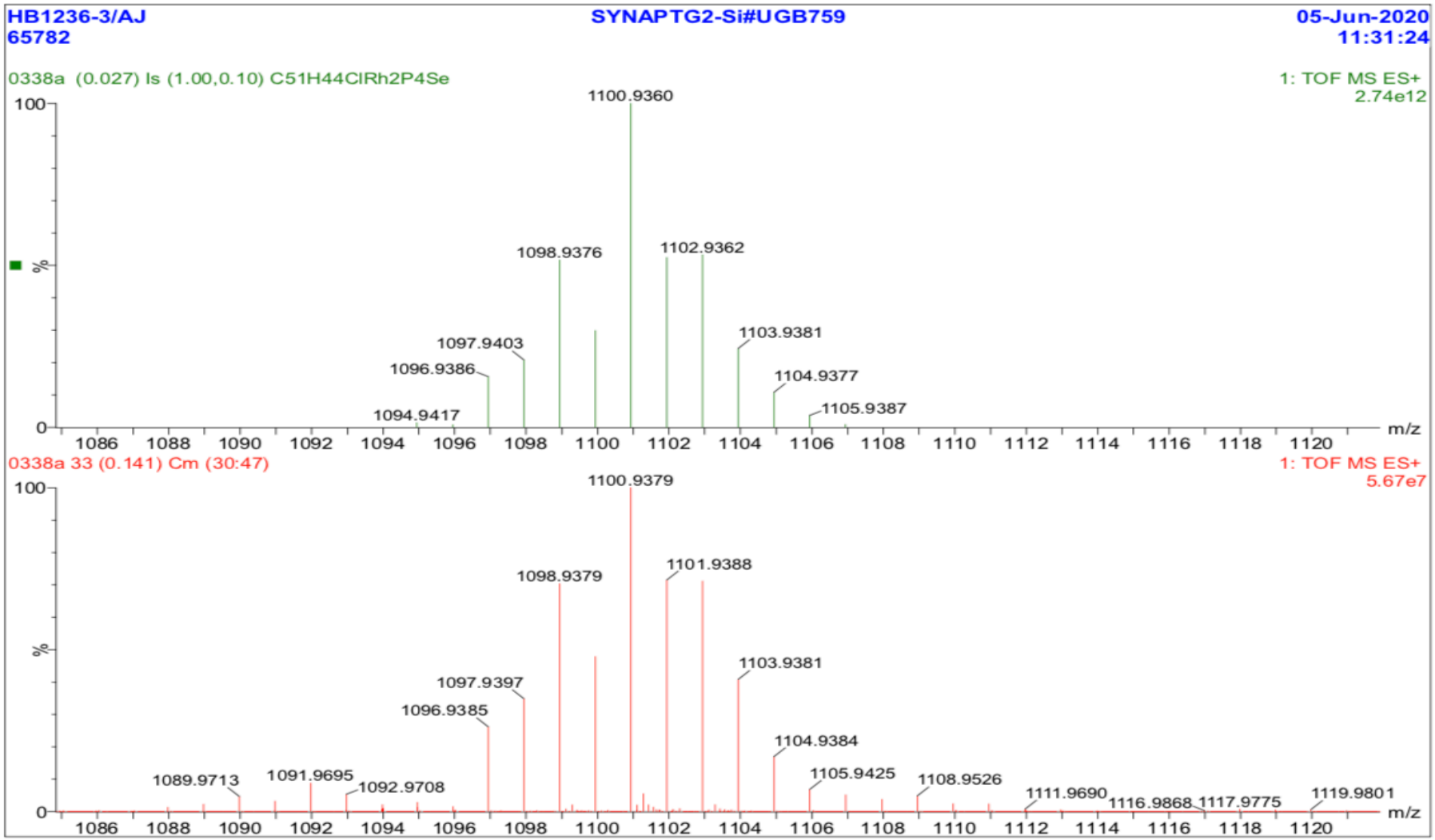

Figure S31. ^{1}H NMR Spectrum of [Rh_2(μ-CS)(μ-DMAD)Cl_2(dppm)$_2$] (7) 600 MHz, 25 °C, $CDCl_3$

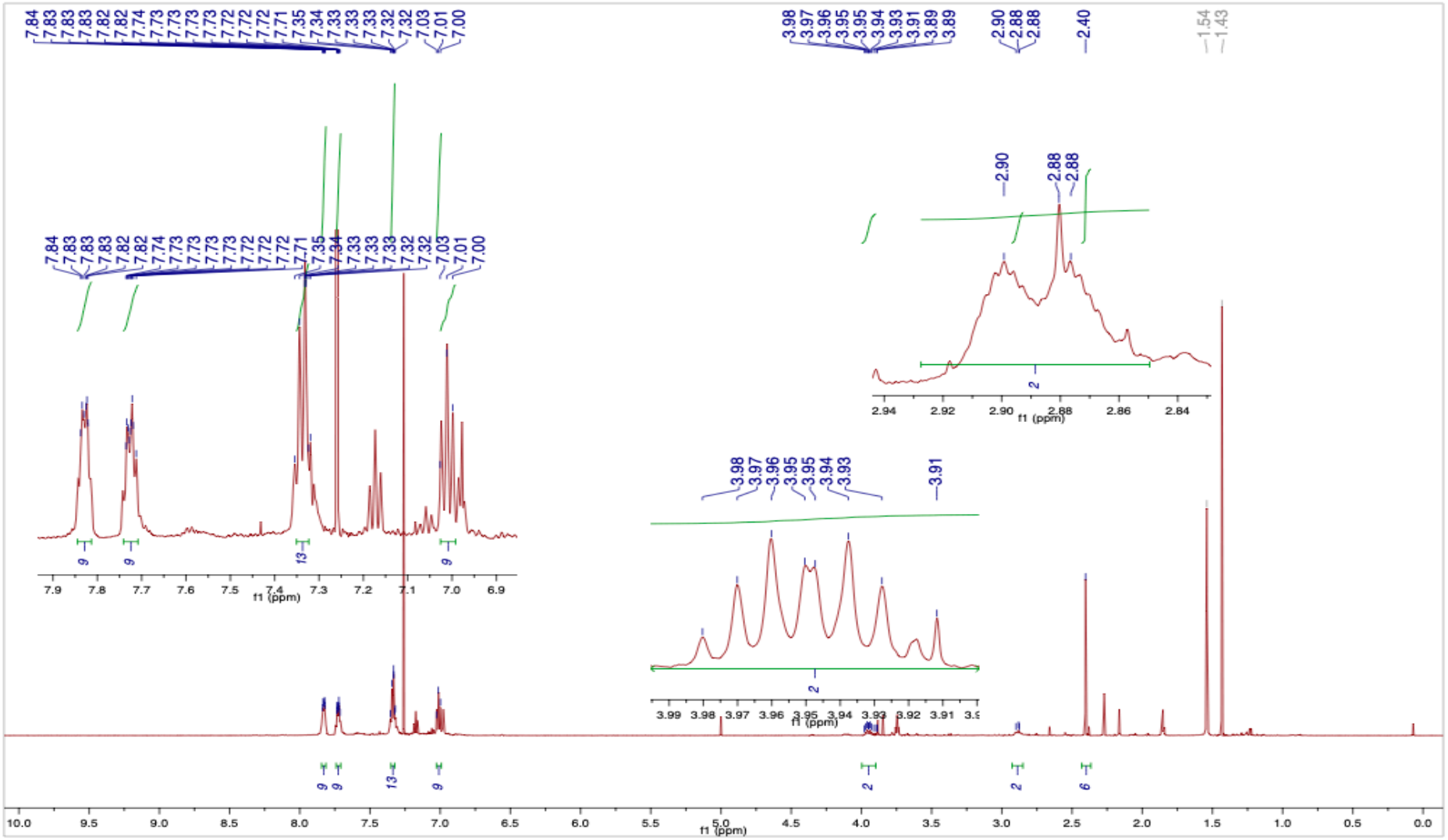

Figure S32. $^{31}P\{^{1}H\}$ NMR Spectrum of $[Rh_2(\mu\text{-}CS)(\mu\text{-}DMAD)Cl_2(dppm)_2]$ (7) 162 MHz, 25 °C, $CDCl_3$

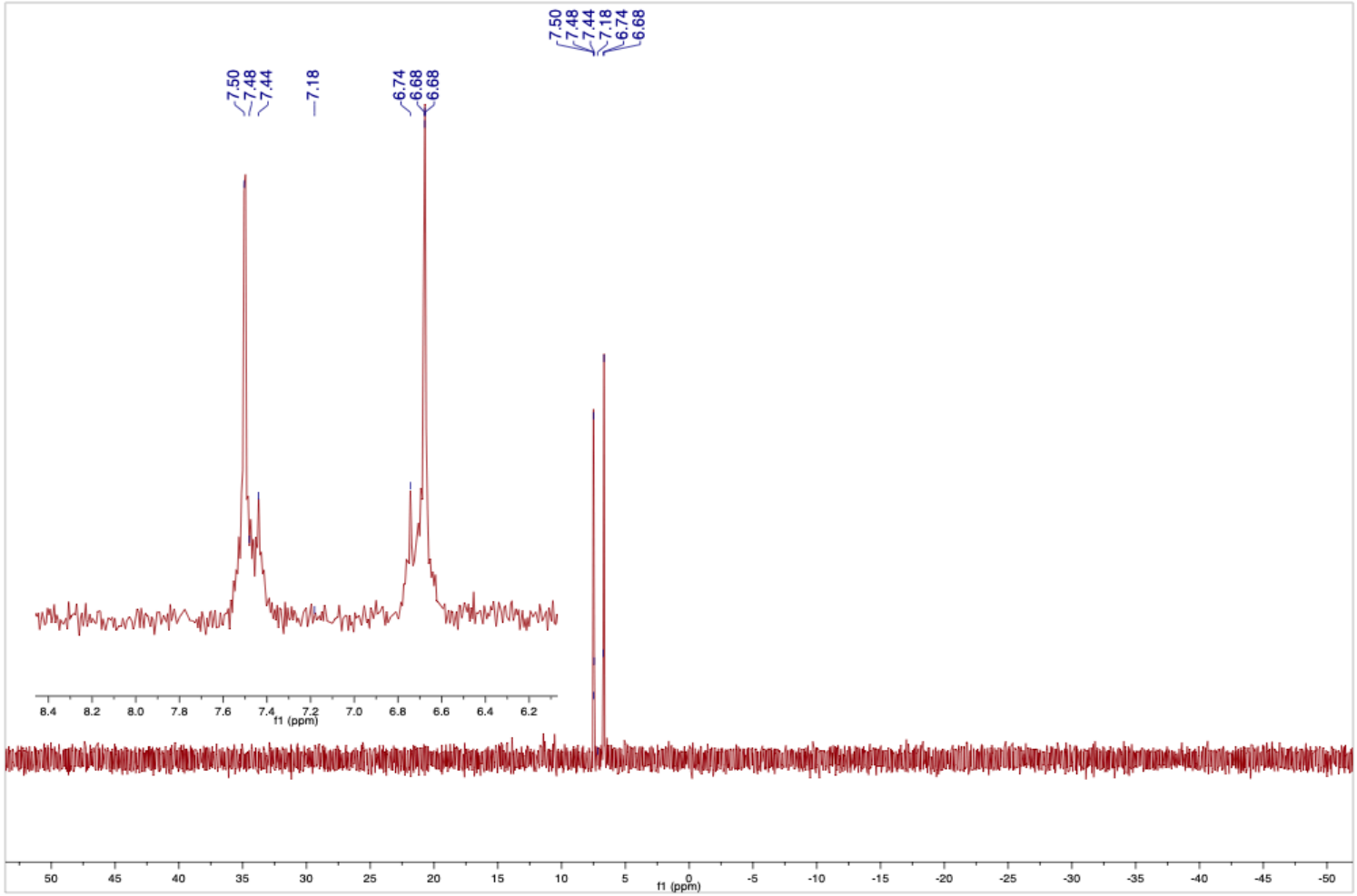

Figure S33. $^{13}C\{^{1}H\}$ **NMR Spectrum** $[Rh_2(\mu\text{-CS})(\mu\text{-DMAD})Cl_2(dppm)_2]$ **(7) 150.9 MHz, 25 °C,** $CDCl_3$

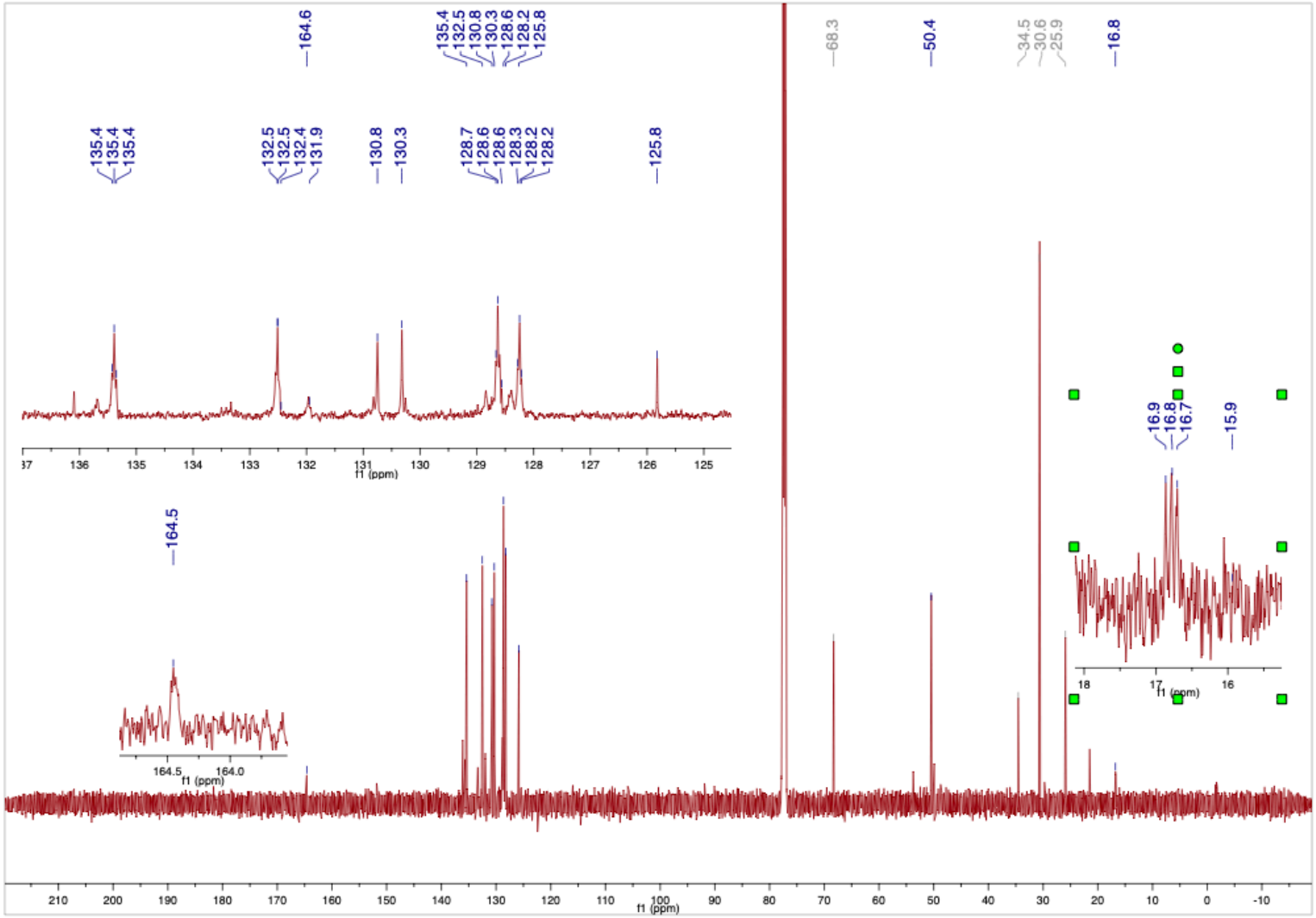

Figure S34. ^{1}H (600 MHz)-^{13}C (151 MHz) HMBC NMR spectrum of $[Rh_2(\mu\text{-}CS)(\mu\text{-}DMAD)Cl_2(dppm)_2]$ (7)

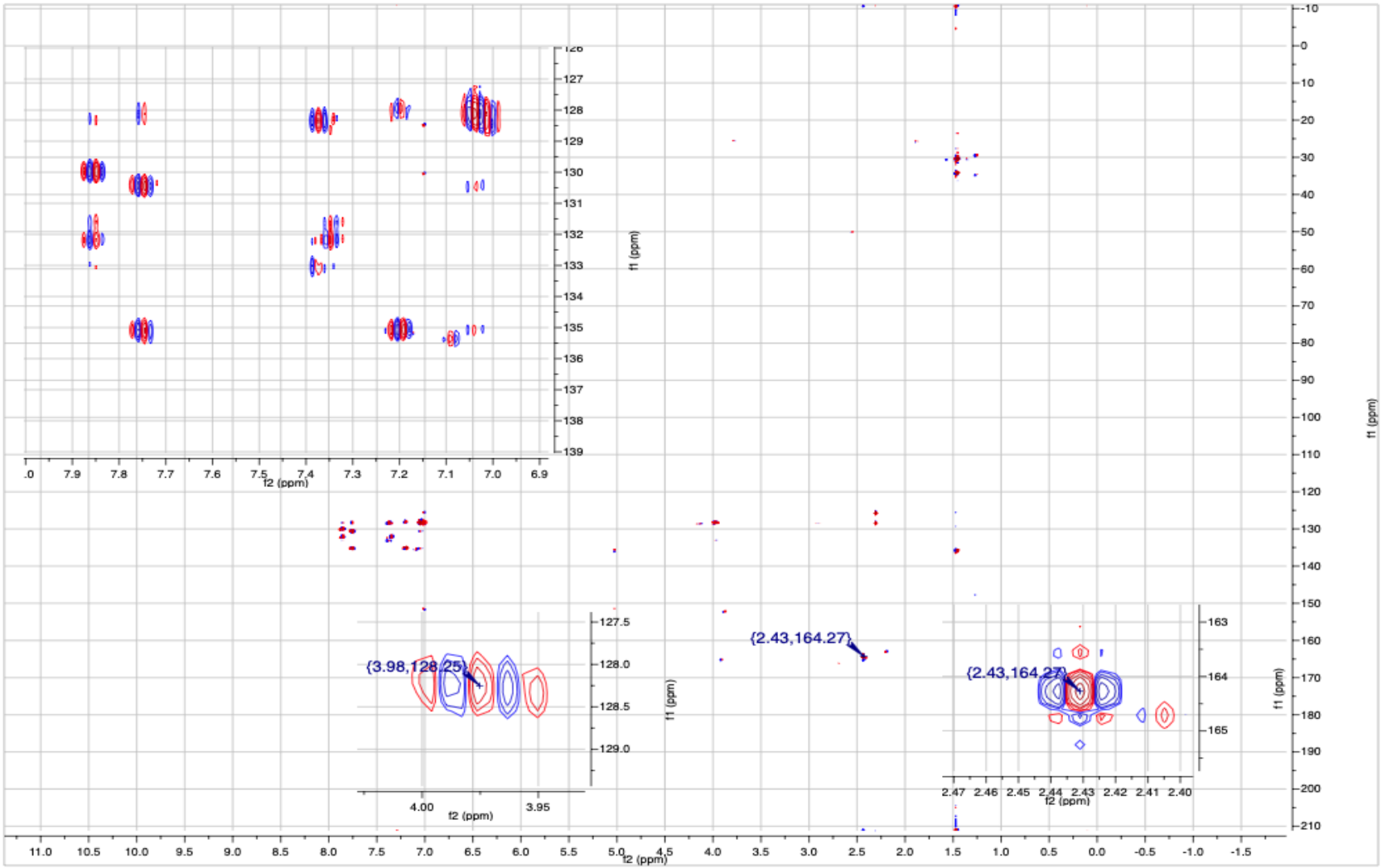

Figure S35. ^{1}H-^{1}H COSY NMR Spectrum of $[Rh_2(\mu\text{-}CS)(\mu\text{-}DMAD)Cl_2(dppm)_2]$ (7) 600 MHz, 25 °C, $CDCl_3$

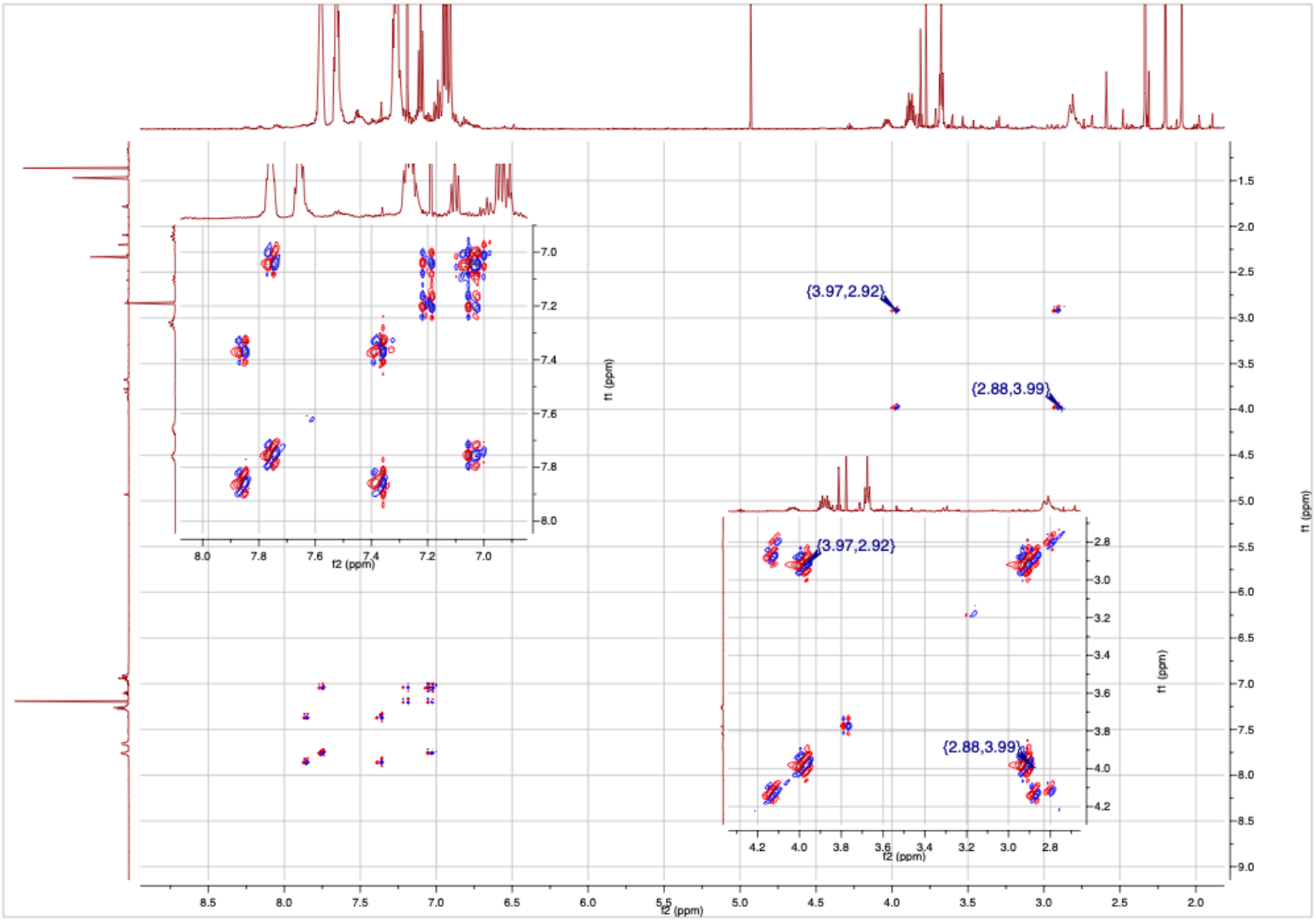

Figure S36. ATR-FT-IR Spectrum of [Rh_2(μ-CS)(μ-DMAD)Cl_2(μ-dppm)$_2$] (7)

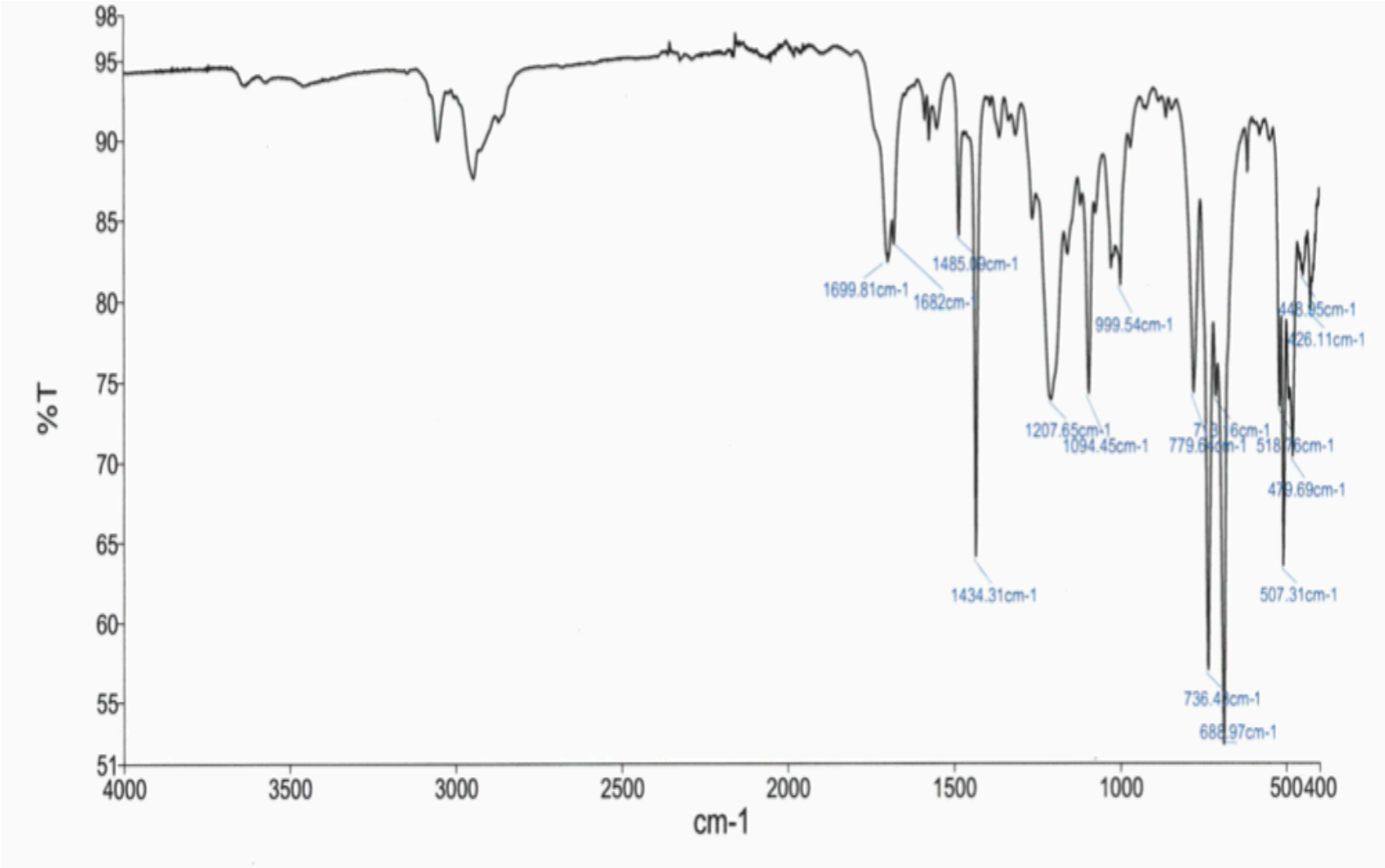

Figure S37. ESI-MS (accurate mass) Spectrum of [Rh_2(μ-CS)(μ-DMAD)Cl_2(μ-dppm)$_2$] (7)

Single Mass Analysis
Tolerance = 3.0 PPM / DBE: min = -1.5, max = 35.0
Element prediction: Off
Number of isotope peaks used for i-FIT = 3

Monoisotopic Mass, Even Electron Ions
560 formula(e) evaluated with 1 results within limits (up to 50 best isotopic matches for each mass)
Elements Used:
C: 0-60 H: 0-60 O: 0-4 P: 0-4 S: 0-1 35Cl: 0-1 37Cl: 0-1 103Rh: 0-2
HB-1234-1/AJ
0065 32 (0.138) Cm (29:40)

1: TOF MS ES+
4.66e+005

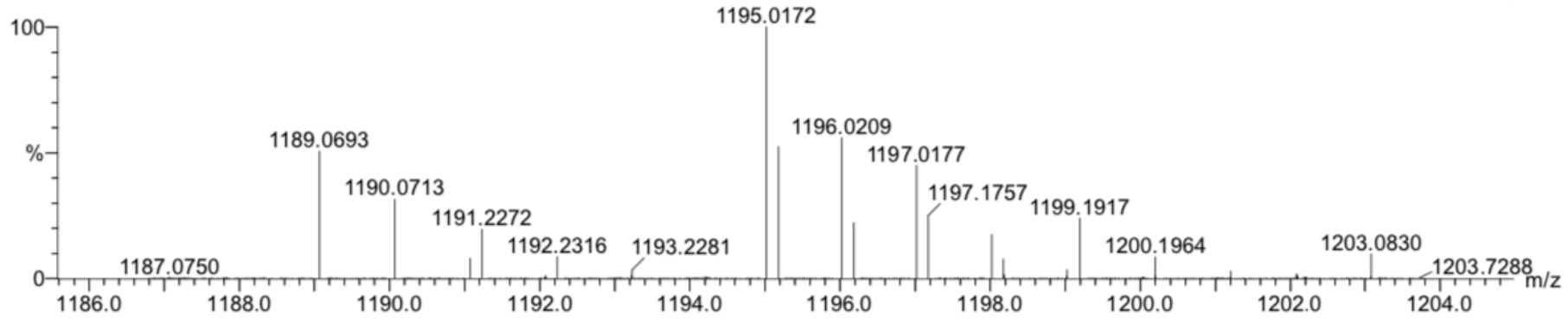

Minimum:				-1.5				
Maximum:		5.0	3.0	35.0				
Mass	Calc. Mass	mDa	PPM	DBE	i-FIT	Norm	Conf(%)	Formula
1195.0172	1195.0179	-0.7	-0.6	34.5	790.5	n/a	n/a	C57 H50 O4 P4 S 35Cl 103Rh2

Figure S38. ^{1}H NMR Spectrum of [Rh_2(μ-CSe)(μ-DMAD)Cl_2(μ-dppm)$_2$] (8)

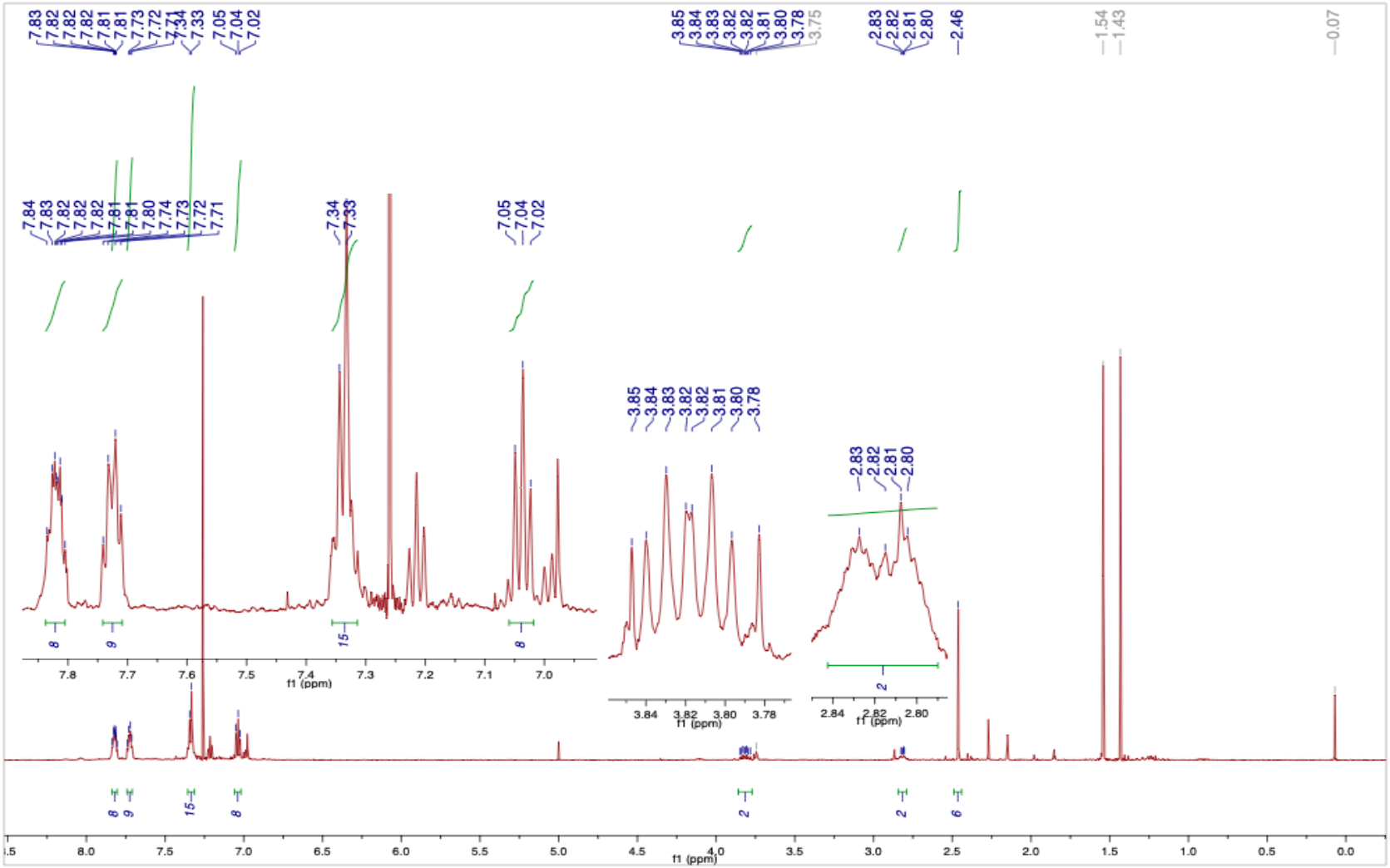

Figure S39. $^{31}P\{^{1}H\}$ **NMR Spectrum of** $[Rh_2(\mu\text{-CSe})(\mu\text{-DMAD})Cl_2(\mu\text{-dppm})_2]$ **(8) 162 MHz, 25 °C,** $CDCl_3$

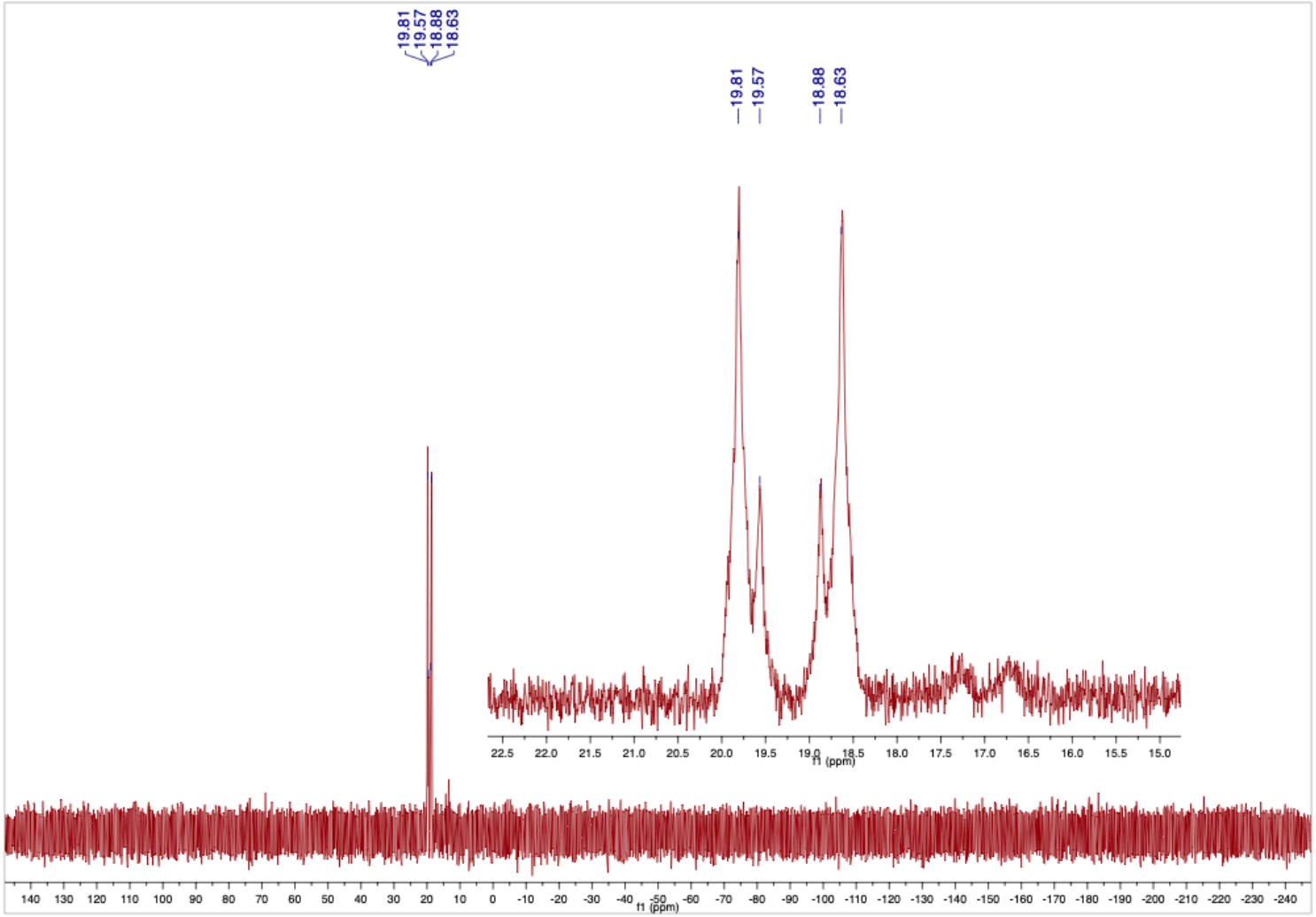

Figure S40. $^{13}C\{^{1}H\}$ NMR Spectrum of $[Rh_2(\mu\text{-CSe})(\mu\text{-DMAD})Cl_2(\mu\text{-dppm})_2]$ (8) 151 MHz, 25 °C, $CDCl_3$

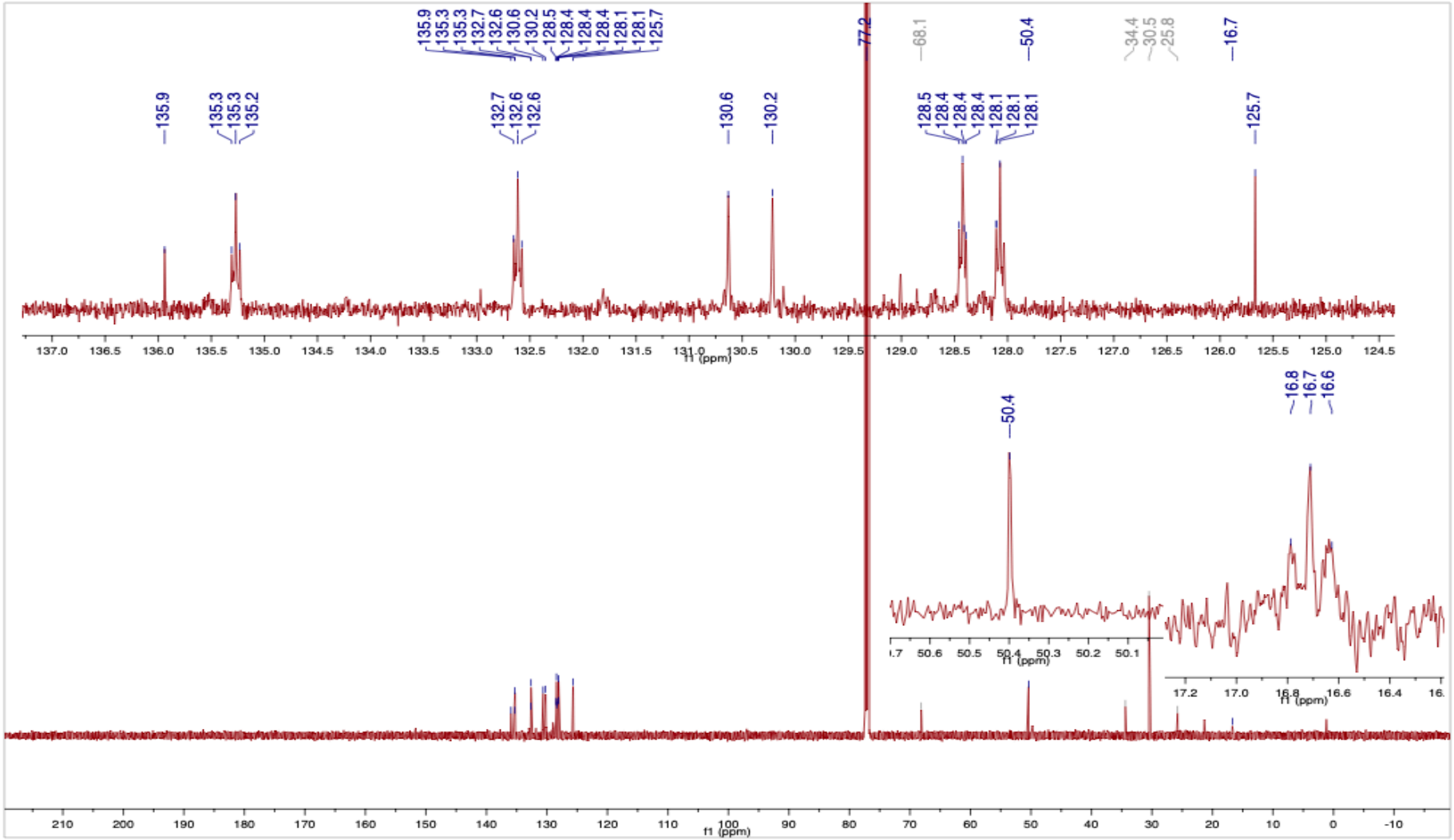

Figure S41. $^{77}Se\{^{1}H\}$ NMR Spectrum of $[Rh_2(\mu\text{-CSe})(\mu\text{-DMAD})Cl_2(\mu\text{-dppm})_2]$ (8) δ(CSe) not identified

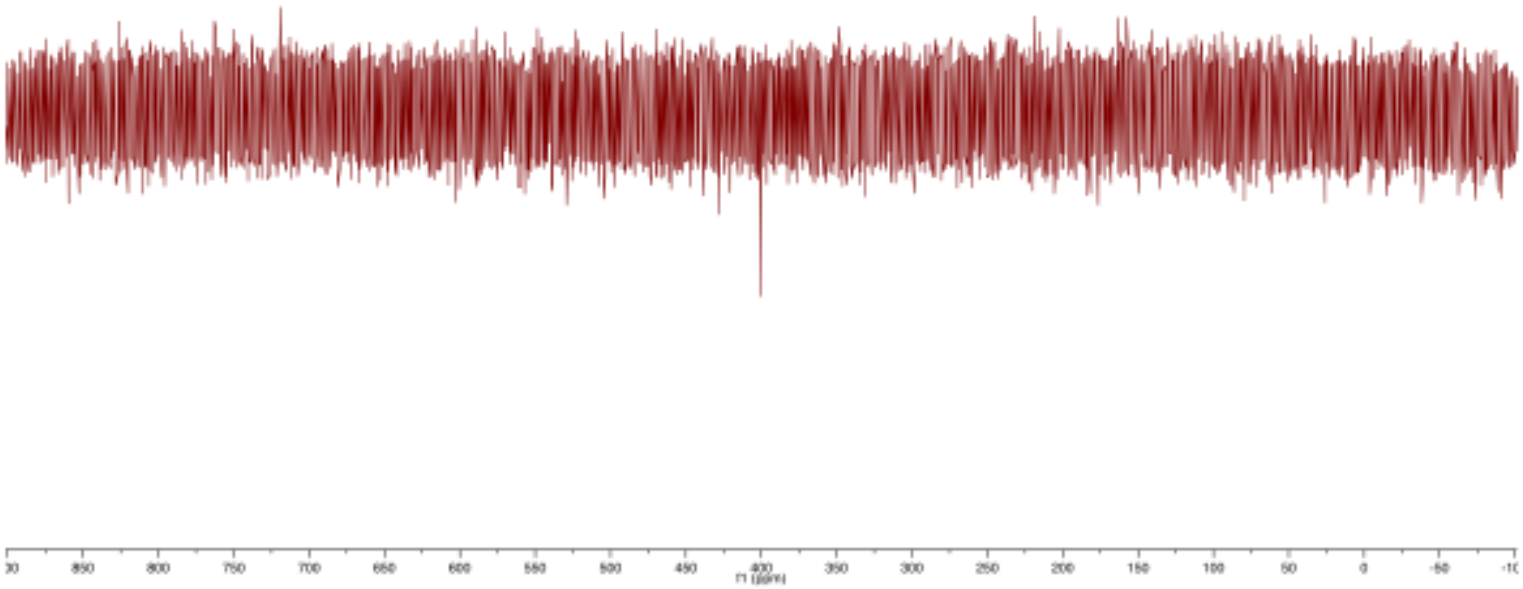

Figure S42. ^{1}H (600 MHz)-^{13}C (151 MHz) HMBC NMR spectrum of [Rh$_2$(μ-CSe)(μ-DMAD)Cl$_2$(μ-dppm)$_2$] (8)

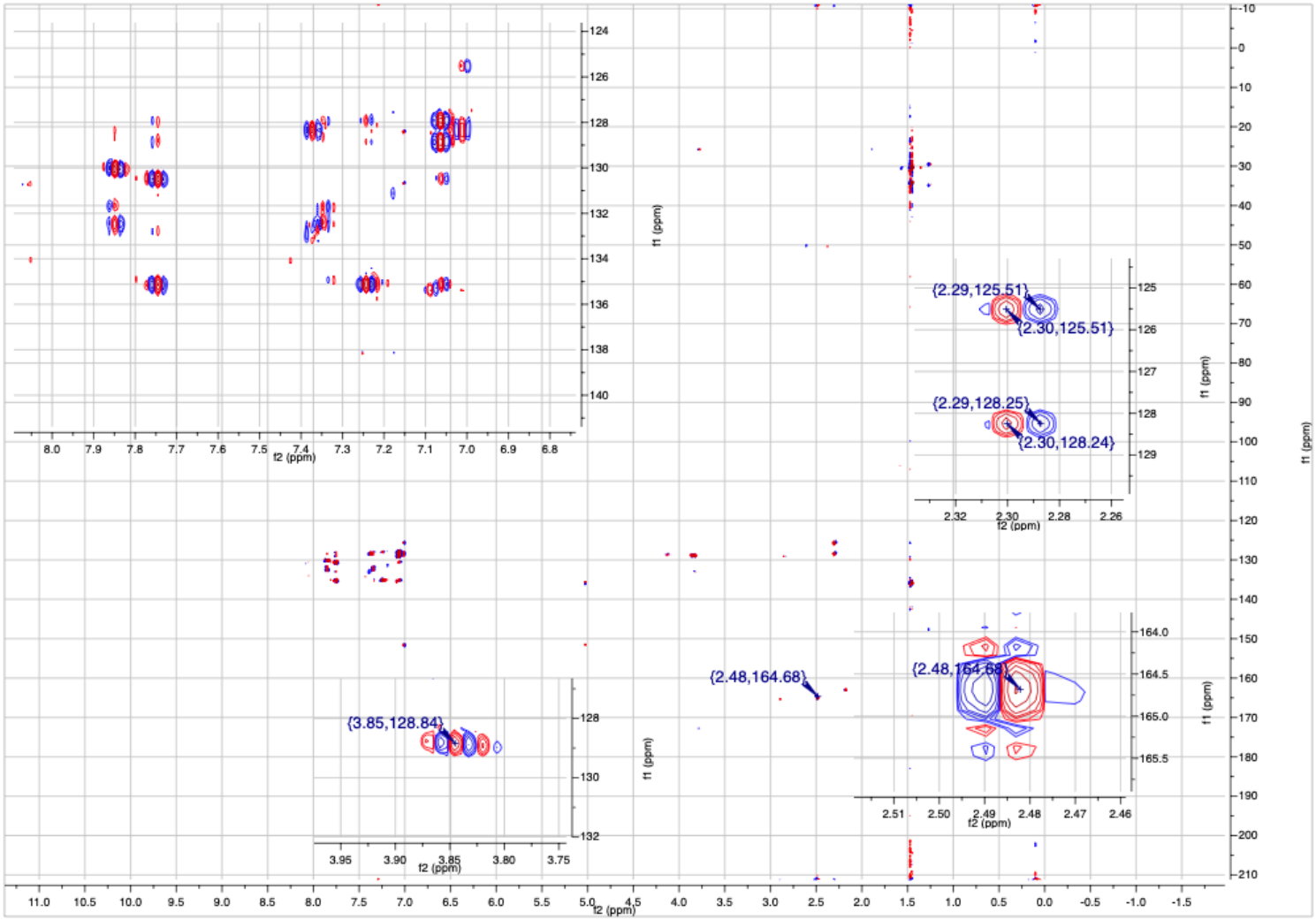

Figure S43. ^{1}H(600 MHz)-^{13}C(151 MHz) HSQC NMR Spectrum of [Rh_2(μ-CSe)(μ-DMAD)Cl_2(μ-dppm)$_2$] (8) 25 °C, $CDCl_3$

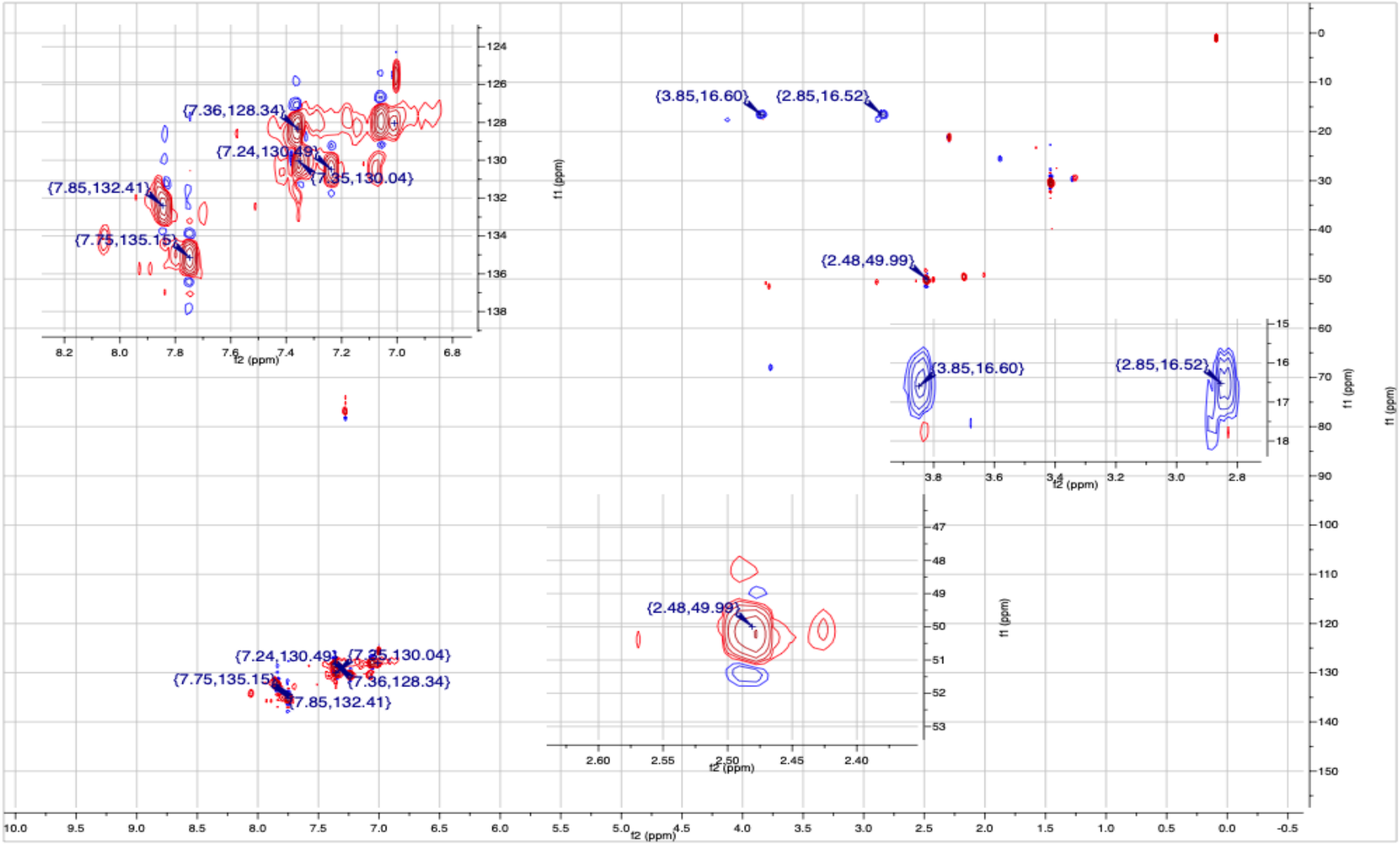

Figure S44. COSY NMR Spectrum of $[Rh_2(\mu\text{-CSe})(\mu\text{-DMAD})Cl_2(\mu\text{-dppm})_2]$ (8) 600 MHz, 25 °C, $CDCl_3$

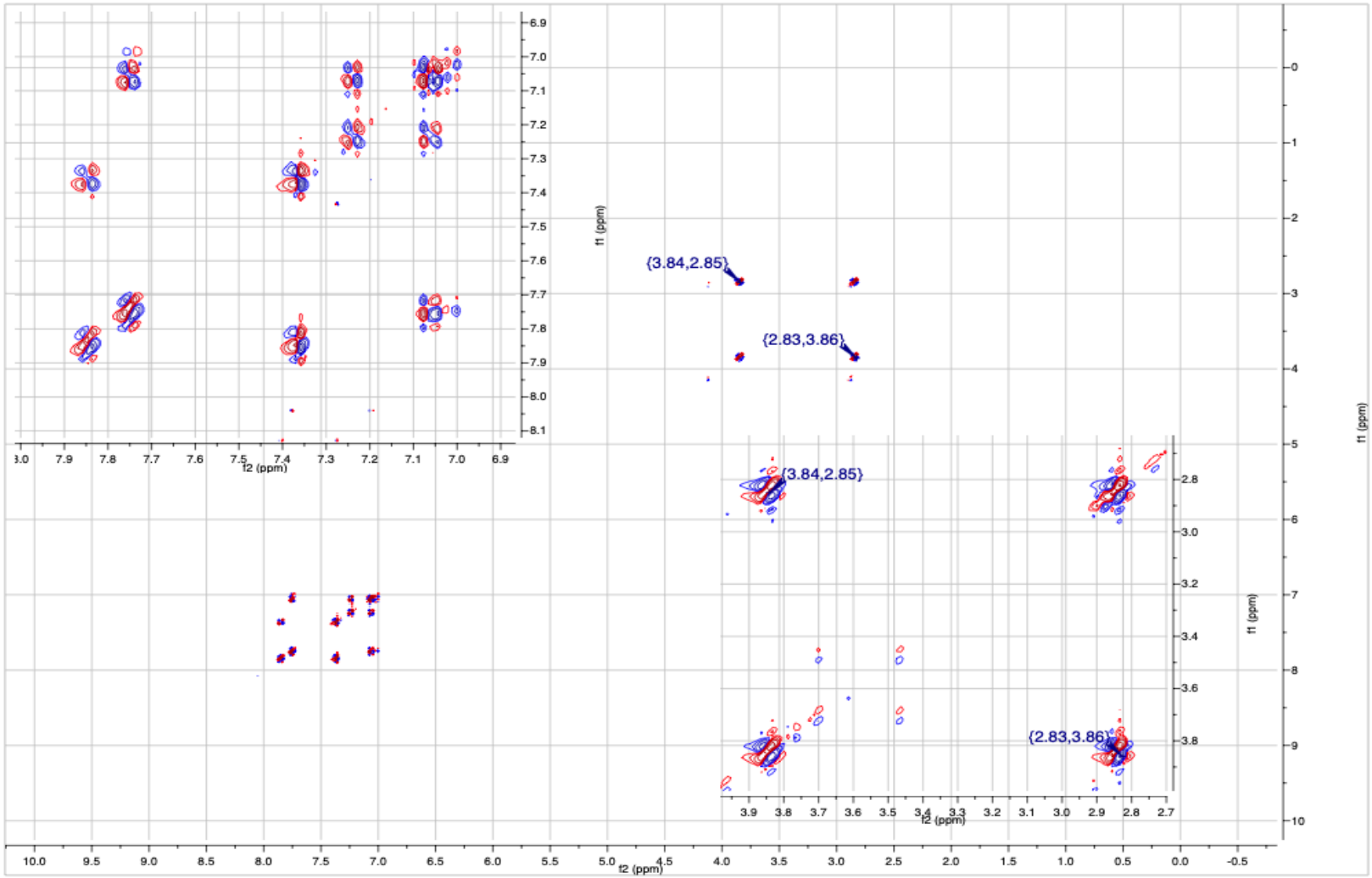

Figure S45. ATR-FT-IR Spectrum of [Rh_2(μ-CSe)(μ-DMAD)Cl_2(μ-dppm)$_2$] (8)

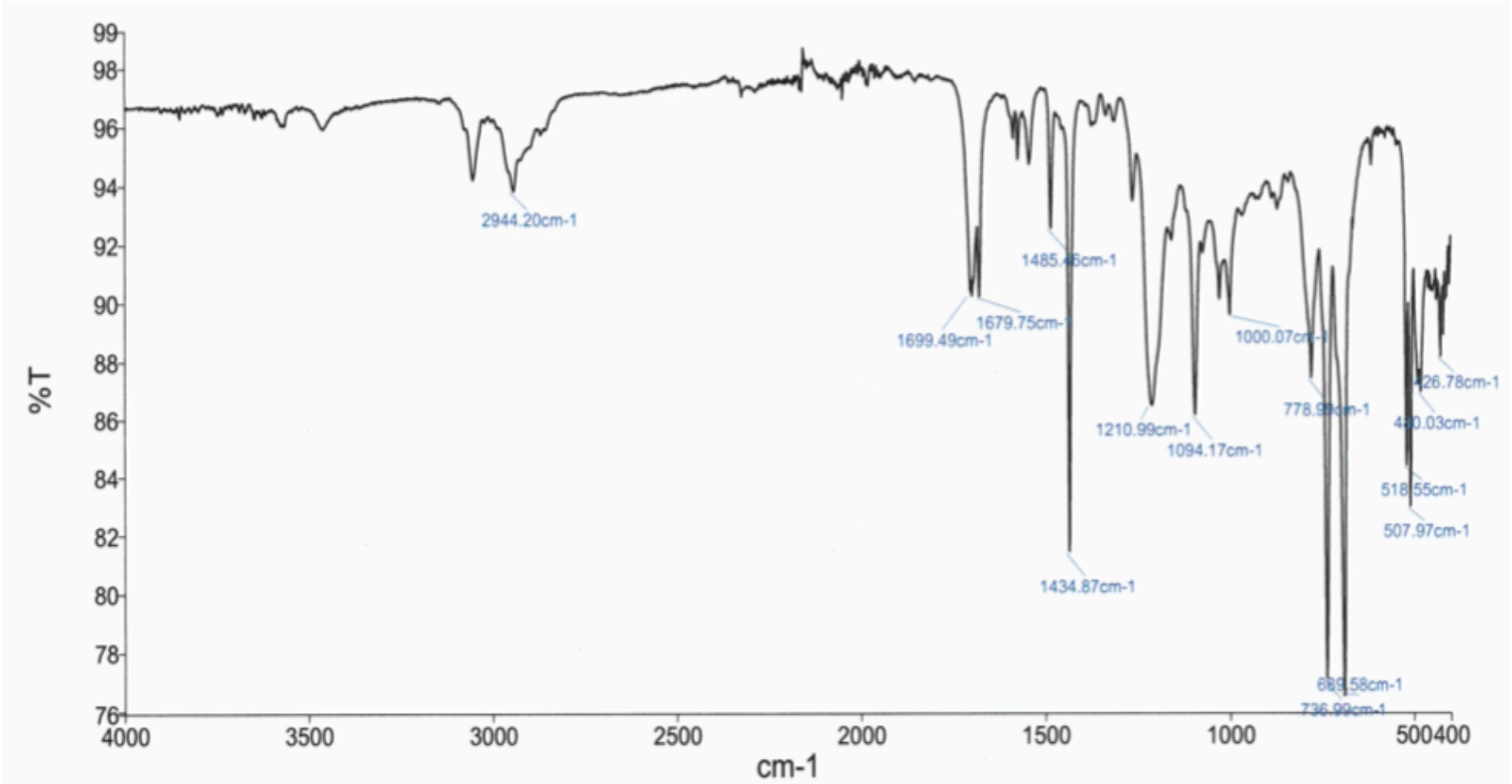

Figure S46. ESI-MS Spectrum of $[Rh_2(\mu\text{-CSe})(\mu\text{-DMAD})Cl_2(\mu\text{-dppm})_2]$ (8)

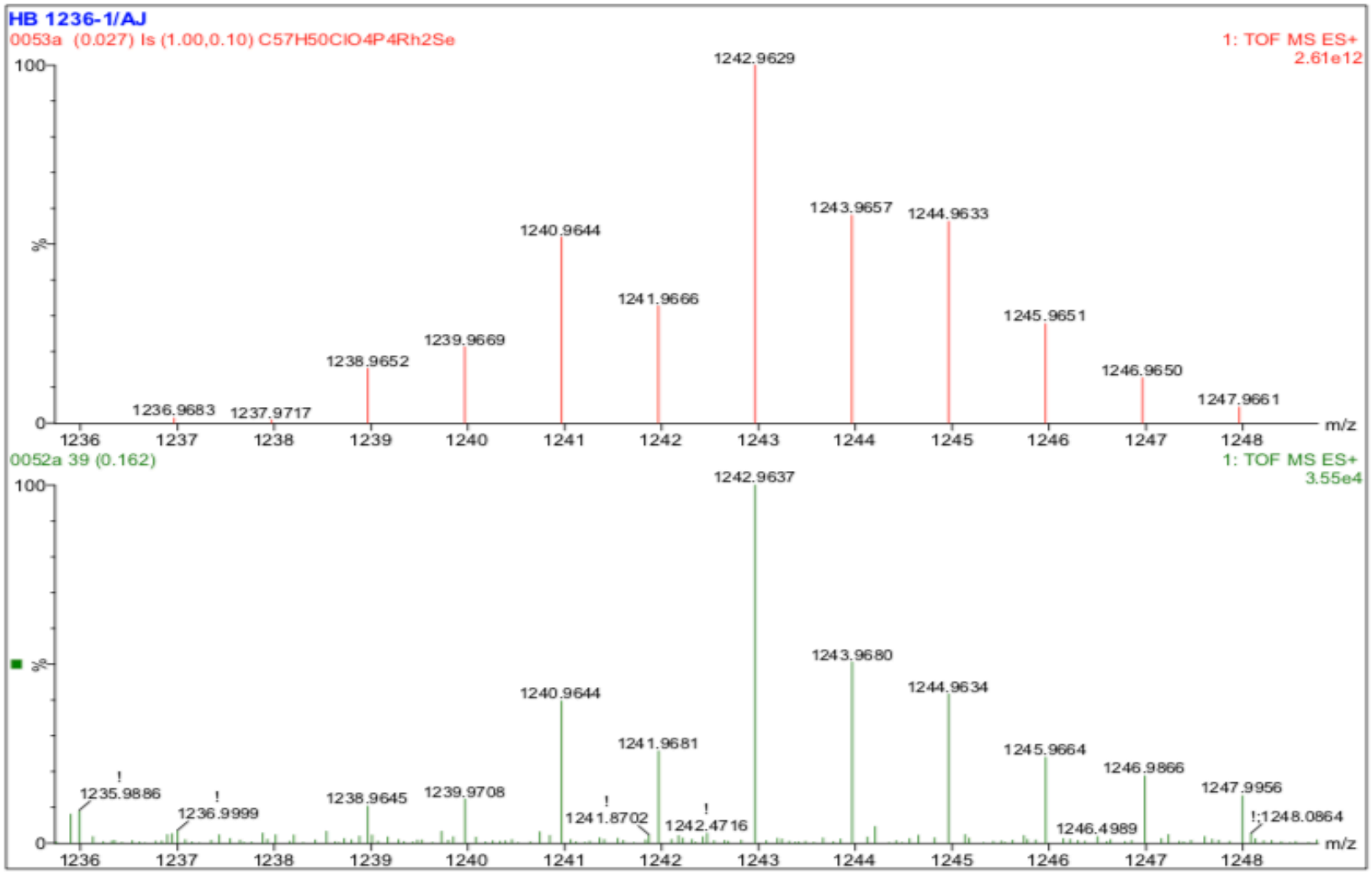

Figure S47. ^{1}H NMR Spectrum of [RhCl(CS)(PPh$_3$)$_2$] (2)

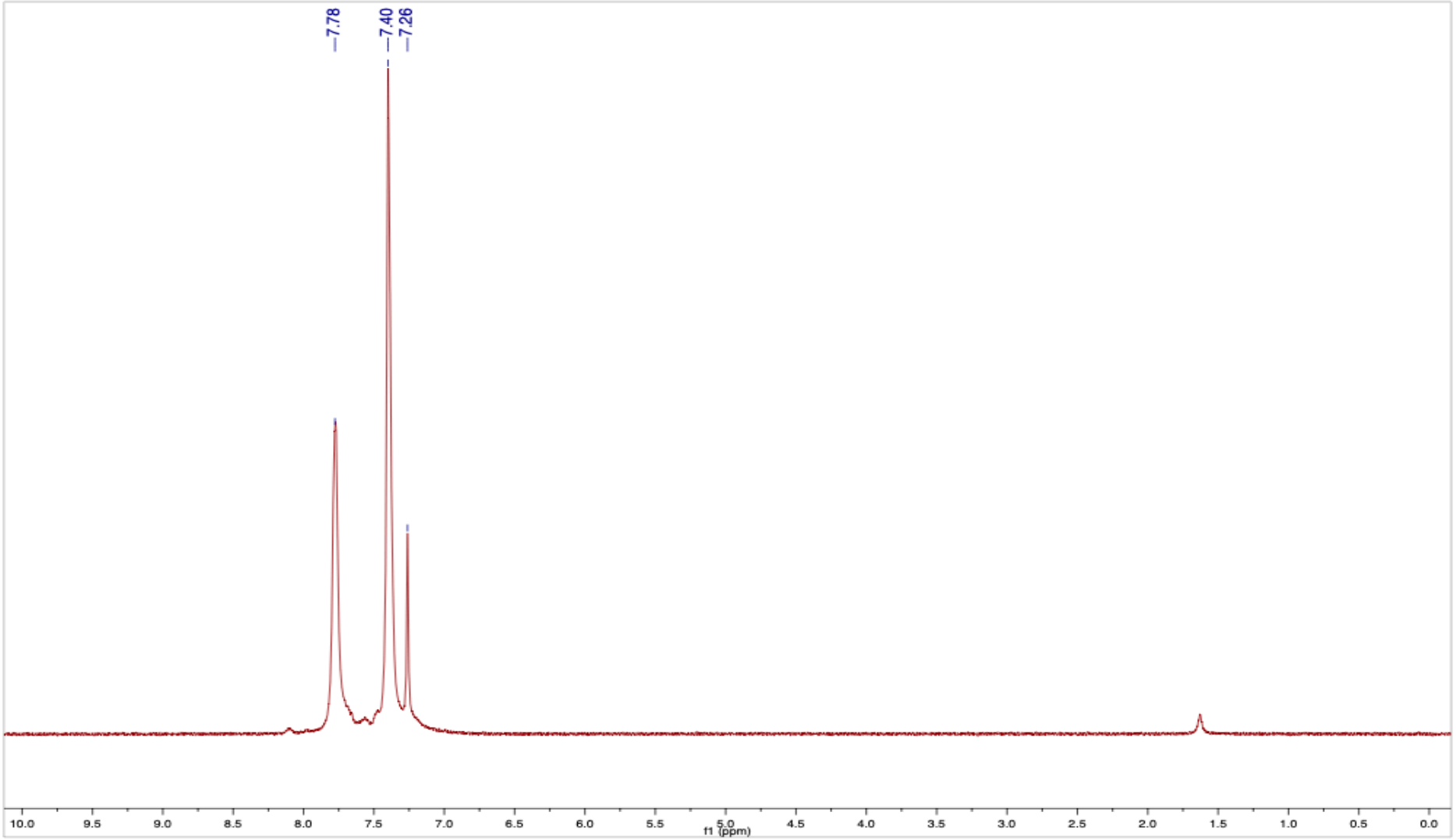

Figure S48. $^{13}C\{^{1}H\}$ NMR Spectrum (20% ^{13}C enrichment of CS, 100.7 MHz, $CDCl_3$, 25 °C) of $[RhCl(CS)(PPh_3)_2]$ (2).

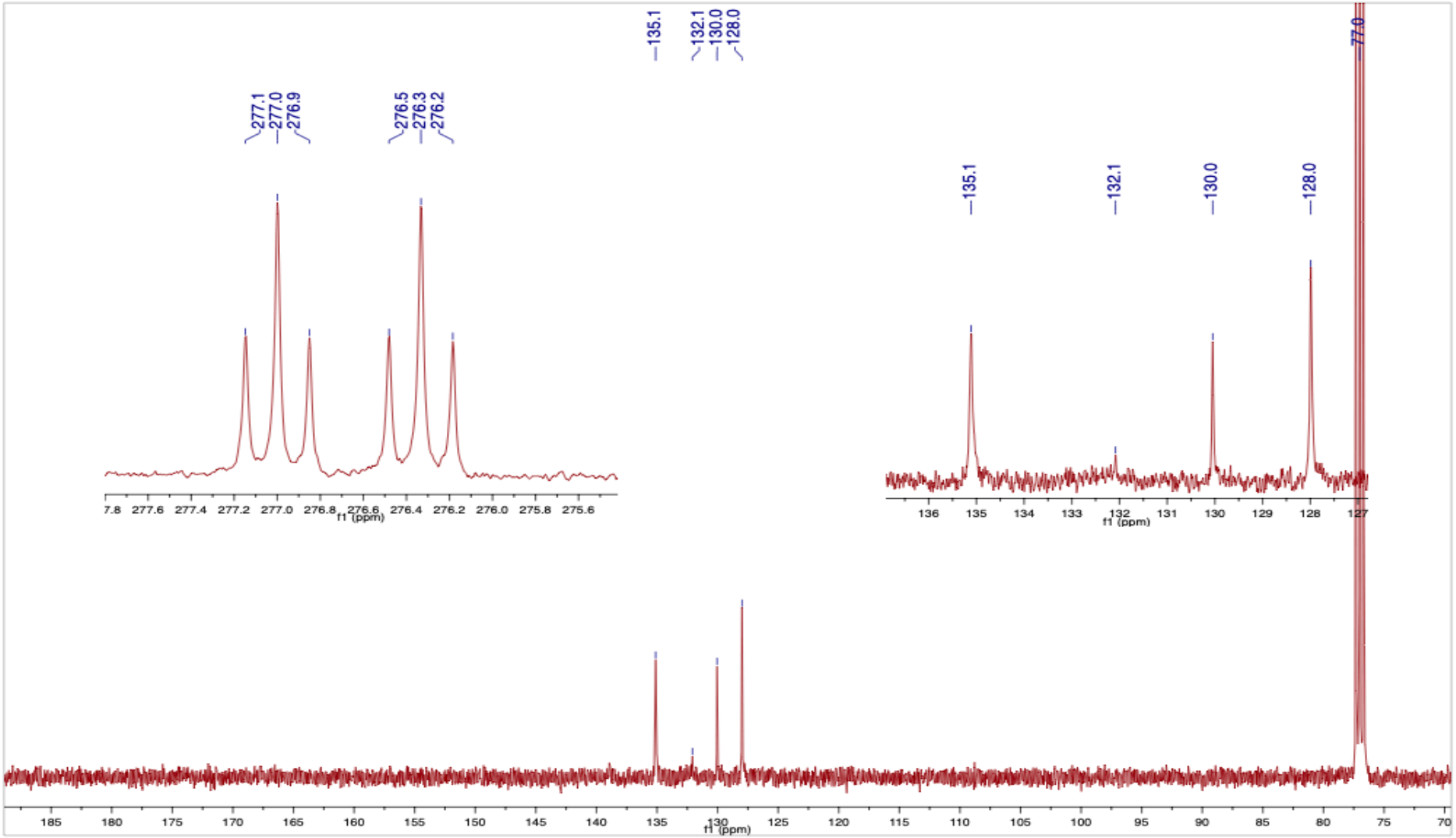

Figure S49. $^{31}P\{^{1}H\}$ NMR Spectrum (20% ^{13}C enriched CS, 162.0 MHz, $CDCl_3$, 25 °C) of $[RhCl(CS)(PPh_3)_2]$ (2)